REPORT ON A HELICOPTER-BORNE VERSATILE TIME DOMAIN ELECTROMAGNETIC (VTEM^{plus}) AND HORIZONTAL MAGNETIC GRADIOMETER GEOPHYSICAL SURVEY

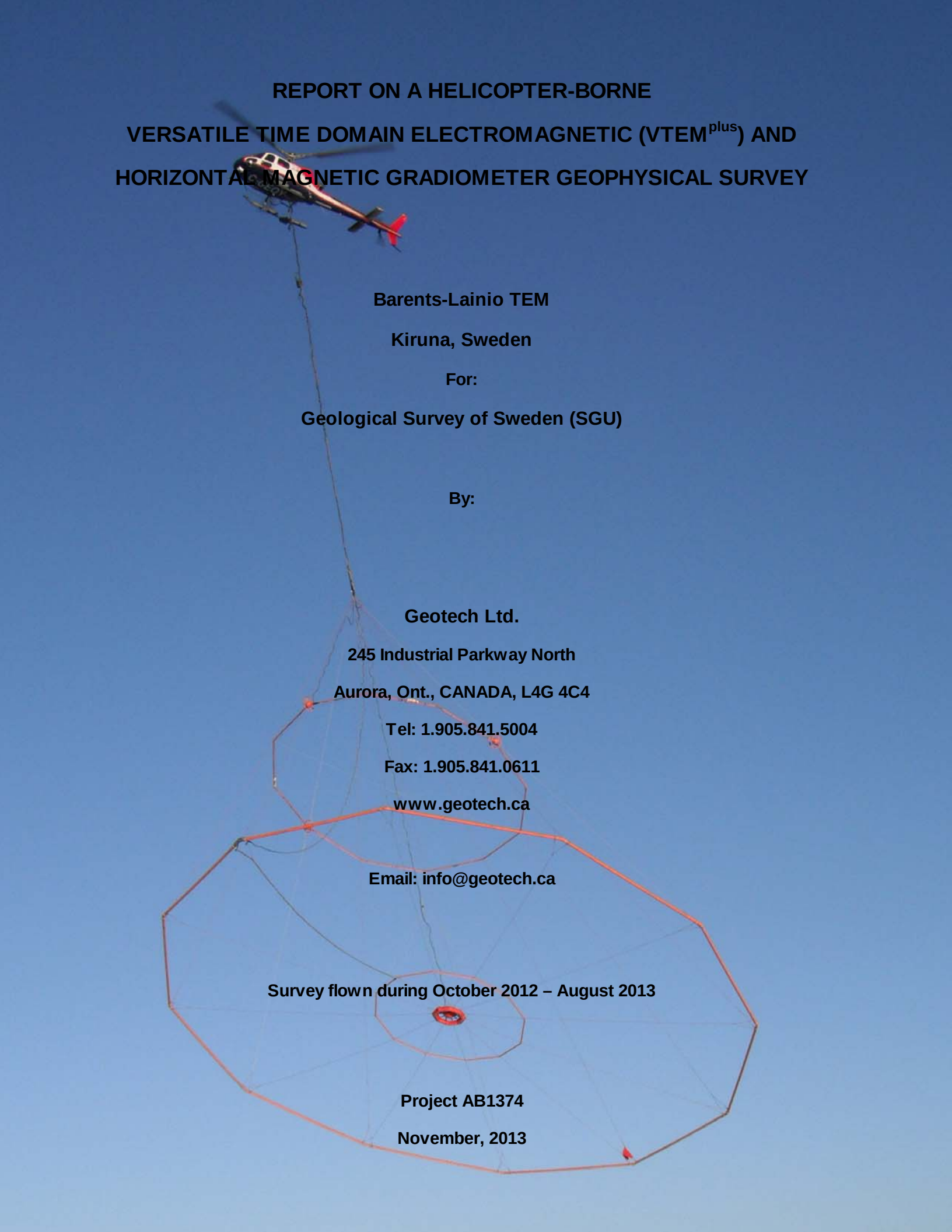

Barents-Lainio TEM

Kiruna, Sweden

For:

Geological Survey of Sweden (SGU)

By:

Geotech Ltd.

245 Industrial Parkway North

Aurora, Ont., CANADA, L4G 4C4

Tel: 1.905.841.5004

Fax: 1.905.841.0611

www.geotech.ca

Email: info@geotech.ca

Survey flown during October 2012 – August 2013

Project AB1374

November, 2013

TABLE OF CONTENTS

LIST OF FIGURES

LIST OF TABLES

APPENDICES

REPORT ON A HELICOPTER-BORNE VERSATILE TIME DOMAIN ELECTROMAGNETIC (VTEM^{plus}) and HORIZONTAL MAGNETIC GRADIOMETER GEOPHYSICAL SURVEY

Barents-Lainio TEM
Kiruna, Sweden

EXECUTIVE SUMMARY

During October 23rd, 2012 to August 30th 2013 Geotech Ltd. carried out a helicopter-borne geophysical survey over the Barents-Lainio TEM block situated near KIruna, Sweden.

Principal geophysical sensors included a versatile time domain electromagnetic (VTEM^{plus}) system, and horizontal magnetic gradiometer. Ancillary equipment included a GPS navigation system and a radar altimeter. A total of 4531 line-kilometres of geophysical data were acquired during the survey.

In-field data quality assurance and preliminary processing were carried out on a daily basis during the acquisition phase. Preliminary and final data processing, including generation of final digital data and map products were undertaken from the office of Geotech Ltd. in Aurora, Ontario.

The processed survey results are presented as the following maps:

- Electromagnetic stacked profiles of the B-field Z Component,
- Electromagnetic stacked profiles of dB/dt Z Components,
- B-Field Z Component Channel grid
- Total Magnetic Intensity (TMI),
- Fraser Filtered dB/dt X Component Channel grid,
- Magnetic Total Horizontal Gradient
- Magnetic Tilt-Angle Derivative
- Calculated Time Constant (Tau) with contours of anomaly areas of the Calculated Vertical Derivative of TMI
- RDI sections are presented.

Digital data includes all electromagnetic and magnetic products, plus ancillary data including the waveform.

The survey report describes the procedures for data acquisition, processing, final image presentation and the specifications for the digital data set.

1. INTRODUCTION

1.1 General Considerations

Geotech Ltd. performed a helicopter-borne geophysical survey over Barents-Lainio TEM block located near Kiruna, Sweden (Figure 1 & 2).

Kajsa Hult represented the Geological Survey of Sweden (SGU) during the data acquisition and data processing phases of this project.

The geophysical surveys consisted of helicopter borne EM using the versatile time-domain electromagnetic (VTEM^{plus}) full receiver-waveform streamed data recorded system with Z and X component measurements and horizontal magnetic gradiometer using two cesium magnetometers. A total of 4531 line-km of geophysical data were acquired during the survey.

The crew was based out of Kiruna (Figure 2) in Sweden for the acquisition phase of the survey. Survey flying started on October 23rd 2012 and was completed on August 30th, 2013.

Data quality control and quality assurance, and preliminary data processing were carried out on a daily basis during the acquisition phase of the project. Final data processing followed immediately after the end of the survey. Final reporting, data presentation and archiving were completed from the Aurora office of Geotech Ltd. in November, 2013.

Figure 1: Property Location.

1.2 Survey and System Specifications

The block is located approximately 15 kilometres north of Kiruna, Sweden (Figure 2).

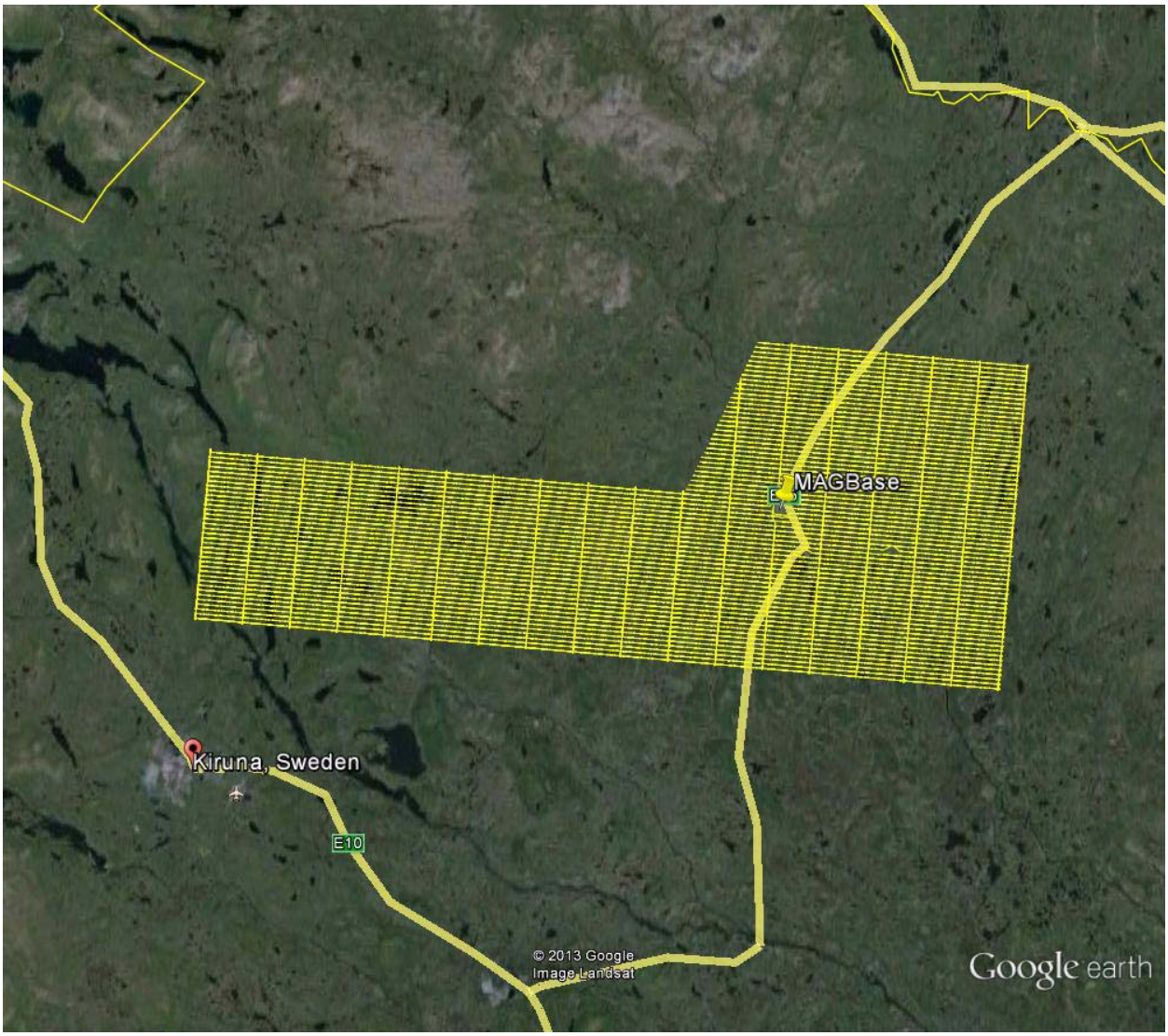

Figure 2: Survey area location on Google Earth.

The block was flown in an East to West (N 95° E azimuth) direction traverse line spacing of 500 metres as depicted in Figure 3. Tie lines were flown perpendicular to the traverse lines at a spacing of 4985 metres respectively. For more detailed information on the flight spacing and direction see Table 1.

1.3 Topographic Relief and Cultural Features

Topographically, the block exhibits a moderate relief with an elevation ranging from 323 to 822 metres above mean sea level over an area of 2088 square kilometres (Figure 3).

There are various rivers and streams running through the survey area which connect various lakes. There are visible signs of culture such as roads and powerlines as well as small settlements which run throughout the survey. There is also a military firing ground in the middle of the block.

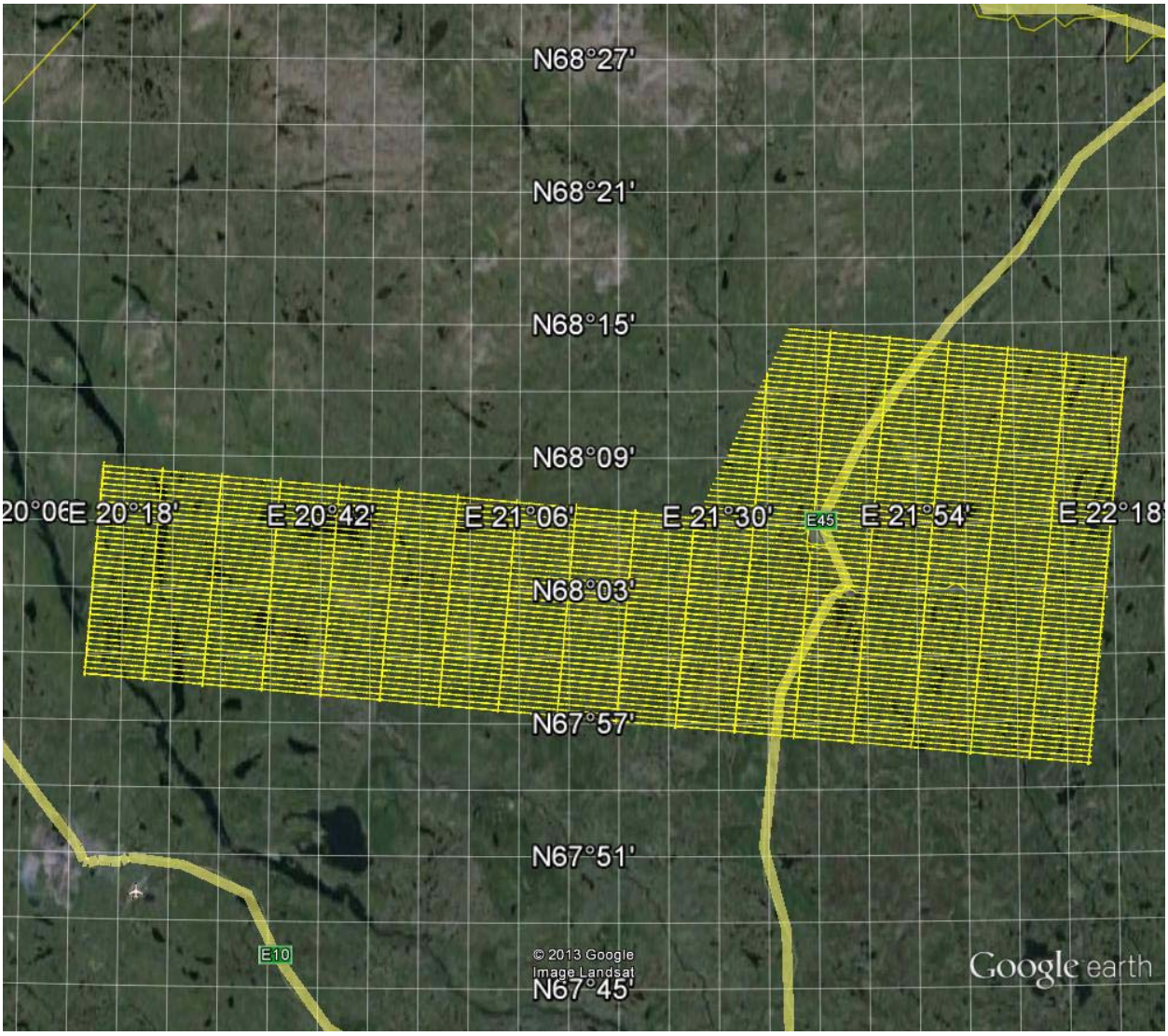

Figure 3: Flight path over a Google Earth Image

2. DATA ACQUISITION

2.1 Survey Area

The survey block (see Figure 3 and Appendix A) and general flight specifications are as follows:

Table 1: Survey Specifications

Survey block	Traverse Line spacing (m)	Area (Km^2)	Planned[1] Line-km	Actual Line-km	Flight direction	Line numbers
block	Traverse: 500	2088	4531	4611.7	N 95° E / N 275° E	L1000-L1681
	Tie: 4985				N 5° E / N 185° E	T1800-T1970
TOTAL		**2088**	**4531**	**4611.7**		

Survey block boundaries co-ordinates are provided in Appendix B.

2.2 Survey Operations

Survey operations were based out of Ovre Soppero in Sweden from October 23rd, 2012 to August 30th 2013. The following table shows the timing of the flying.

Table 2: Survey schedule

Date	Flight #	Flow km	Block	Crew location	Comments
23-Oct-2012				Kiruna Sweden	mobilization
24-Oct-2012				Kiruna Sweden	mobilization
25-Oct-2012				Kiruna Sweden	Crew & equipment arrived
26-Oct-2012				Kiruna Sweden	No test flight flown due to weather
27-Oct-2012				Kiruna Sweden	Test flight
28-Oct-2012				Kiruna Sweden	Noise test. Base station setup
29-Oct-2012				Kiruna Sweden	No production due to weather
30-Oct-2012				Kiruna Sweden	No production due to weather
31-Oct-2012				Kiruna Sweden	No production due to weather
1-Nov-2012				Kiruna Sweden	No production due to weather
2-Nov-2012				Kiruna Sweden	No production due to weather
3-Nov-2012				Kiruna Sweden	No production due to weather
4-Nov-2012				Kiruna Sweden	No production due to weather
5-Nov-2012				Kiruna Sweden	No production due to weather
6-Nov-2012				Kiruna Sweden	Project postponed until Spring 2013
25-Jul-2013				Ovre Soppero Sweden	Crew arrived
26-Jul-2013	1,2	173		Ovre Soppero Sweden	173km flown
27-Jul-2013	3,4,5	220		Ovre Soppero Sweden	220km flown
28-Jul-2013				Ovre Soppero Sweden	Pilot Rest Day
29-Jul-2013	6,7	138		Ovre Soppero Sweden	138km flown

[1] Note: Actual Line kilometres represent the total line kilometres in the final database. These line-km normally exceed the planned line-km, as indicated in the survey NAV files.

Date	Flight #	Flow km	Block	Crew location	Comments
30-Jul-2013	8	100		Ovre Soppero Sweden	100km flown
31-Jul-2013	9,10	179		Ovre Soppero Sweden	179km flown
1-Aug-2013	11,12	127		Ovre Soppero Sweden	127km flown
2-Aug-2013				Ovre Soppero Sweden	Pilot Rest Day
3-Aug-2013	13,14	157		Ovre Soppero Sweden	157km flown
4-Aug-2013	15,16	199		Ovre Soppero Sweden	199km flown
5-Aug-2013	17	33		Ovre Soppero Sweden	33km flown limited due to weather
6-Aug-2013	18,19,20	241		Ovre Soppero Sweden	241km flown
7-Aug-2013	21,22	170		Ovre Soppero Sweden	170km flown
8-Aug-2013	23,24,25	280		Ovre Soppero Sweden	280km flown
9-Aug-2013	26,27,28	315		Ovre Soppero Sweden	315km flown
10-Aug-2013	29,30	171		Ovre Soppero Sweden	171km flown
11-Aug-2013	31,32,33	293		Ovre Soppero Sweden	293km flown
12-Aug-2013				Ovre Soppero Sweden	Pilot Rest Day
13-Aug-2013	34,35,36	306		Ovre Soppero Sweden	306km flown
14-Aug-2013	37			Ovre Soppero Sweden	Flight Aborted due to technical issues
15-Aug-2013				Ovre Soppero Sweden	No production due to weather
16-Aug-2013				Ovre Soppero Sweden	No production due to weather
17-Aug-2013				Ovre Soppero Sweden	No production due to weather
18-Aug-2013	38,39,40	255		Ovre Soppero Sweden	255km flown
19-Aug-2013	41	102		Ovre Soppero Sweden	102km flown
20-Aug-2013				Ovre Soppero Sweden	No production due to weather
21-Aug-2013	42	52		Ovre Soppero Sweden	52km flown limited due to weather
22-Aug-2013	43			Ovre Soppero Sweden	Flight aborted due to weather
23-Aug-2013	44,45,46	305		Ovre Soppero Sweden	305km flown
24-Aug-2013	47,48,49	254		Ovre Soppero Sweden	254km flown
25-Aug-2013	50	51		Ovre Soppero Sweden	51km flown limited due to technical issues
26-Aug-2013	51			Ovre Soppero Sweden	No production due to technical issues – test flight
27-Aug-2013	52,53,54	171		Ovre Soppero Sweden	171km flown
28-Aug-2013	55	87		Ovre Soppero Sweden	87km flown
29-Aug-2013	56,57	272		Ovre Soppero Sweden	272km flown
30-Aug-2013	59	36		Ovre Soppero Sweden	Remaining kms were flown – flying complete
				Ovre Soppero Sweden	

2.3 Flight Specifications

During the survey the helicopter was maintained at a mean altitude of 90 metres above the ground with an average survey speed of 80 km/hour. This allowed for an actual average EM bird terrain clearance of 56 metres and a magnetic sensor clearance of 66 metres.

The on board operator was responsible for monitoring the system integrity. He also maintained a detailed flight log during the survey, tracking the times of the flight as well as any unusual geophysical or topographic features.

On return of the aircrew to the base camp the survey data was transferred from a compact flash card (PCMCIA) to the data processing computer. The data were then uploaded via ftp to the Geotech office in Aurora for daily quality assurance and quality control by qualified personnel.

2.4 Aircraft and Equipment

2.4.1 Survey Aircraft

The survey was flown using a Eurocopter Aerospatiale (Astar) SA 315 LAMA helicopter, registration I-EFLY. The helicopter is owned and operated by Air Walser. Installation of the geophysical and ancillary equipment was carried out by a Geotech Ltd crew.

2.4.2 Electromagnetic System

The electromagnetic system was a Geotech Time Domain EM (VTEM^{plus}) full receiver-waveform streamed data recorded system. The "full waveform VTEM system" uses the streamed half-cycle recording of transmitter and receiver waveforms to obtain a complete system response calibration throughout the entire survey flight. VTEM with the Serial number 1 had been used for the survey. The configuration is as indicated in Figure 5.

The VTEM Receiver and transmitter coils were in concentric-coplanar and Z-direction oriented configuration. The receiver system for the project also included a coincident-coaxial X-direction coil to measure the in-line dB/dt and calculate B-Field responses. The EM bird was towed at a mean distance of 34 metres below the aircraft as shown in Figure 5. The VTEM transmitter current waveform is shown diagrammatically in Figure 4.

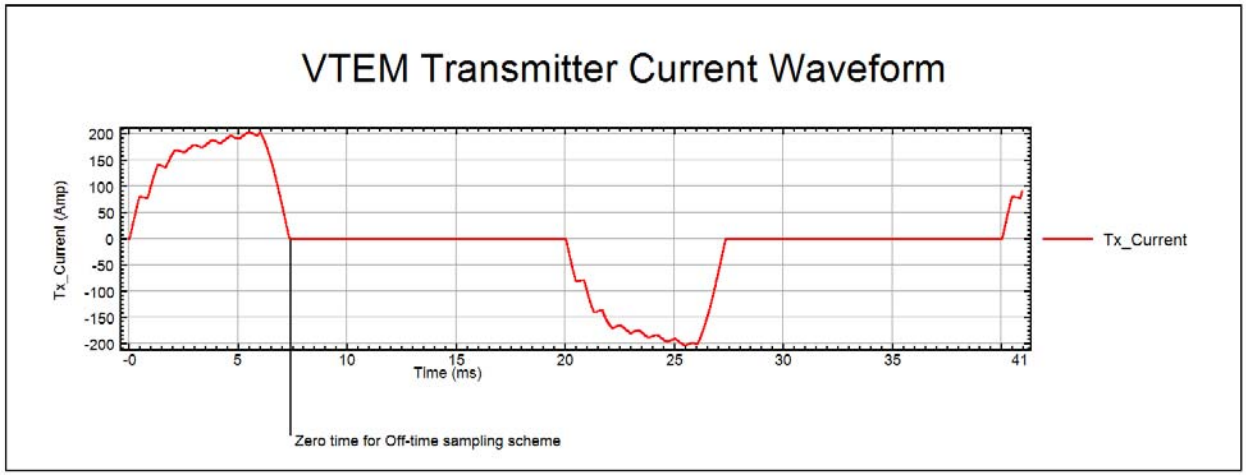

Figure 4: VTEM Transmitter Current Waveform

The VTEM decay sampling scheme is shown in Table 3 below. Forty-five time measurement gates were used for the final data processing in the range from 0.021 to 10.667 msec. Zero time for off-time sampling scheme is equal to current pulse width and defined as the time near the end of the turn-off ramp where the dI/dt waveform falls to 1/2 of its peak value.

Table 3: Off-Time Decay Sampling Scheme

VTEM Decay Sampling Scheme				
index	**Start**	**End**	**Middle**	**Window**
Miliseconds				
4	0.018	0.023	0.021	0.005
5	0.023	0.029	0.026	0.005
6	0.029	0.034	0.031	0.005
7	0.034	0.039	0.036	0.005
8	0.039	0.045	0.042	0.006
9	0.045	0.051	0.048	0.007
10	0.051	0.059	0.055	0.008
11	0.059	0.068	0.063	0.009
12	0.068	0.078	0.073	0.010
13	0.078	0.090	0.083	0.012
14	0.090	0.103	0.096	0.013
15	0.103	0.118	0.110	0.015
16	0.118	0.136	0.126	0.018
17	0.136	0.156	0.145	0.020
18	0.156	0.179	0.167	0.023
19	0.179	0.206	0.192	0.027
20	0.206	0.236	0.220	0.030
21	0.236	0.271	0.253	0.035
22	0.271	0.312	0.290	0.040
23	0.312	0.358	0.333	0.046
24	0.358	0.411	0.383	0.053
25	0.411	0.472	0.440	0.061
26	0.472	0.543	0.505	0.070
27	0.543	0.623	0.580	0.081
28	0.623	0.716	0.667	0.093
29	0.716	0.823	0.766	0.107
30	0.823	0.945	0.880	0.122
31	0.945	1.086	1.010	0.141
32	1.086	1.247	1.161	0.161
33	1.247	1.432	1.333	0.185
34	1.432	1.646	1.531	0.214
35	1.646	1.891	1.760	0.245
36	1.891	2.172	2.021	0.281
37	2.172	2.495	2.323	0.323

VTEM Decay Sampling Scheme				
index	Start	End	Middle	Window
Miliseconds				
38	2.495	2.865	2.667	0.370
39	2.865	3.292	3.063	0.427
40	3.292	3.781	3.521	0.490
41	3.781	4.341	4.042	0.560
42	4.341	4.987	4.641	0.646
43	4.987	5.729	5.333	0.742
44	5.729	6.581	6.125	0.852
45	6.581	7.560	7.036	0.979
46	7.560	8.685	8.083	1.125
47	8.685	9.977	9.286	1.292
48	9.977	11.458	10.667	1.482

Z Component: 4-48 time gates
X Component: 20-48 time gates.

VTEM system specifications:

Transmitter

- Transmitter loop diameter: 26 m
- Number of turns: 4
- Effective Transmitter loop area: 2123.7 m^2
- Transmitter base frequency: 25 Hz
- Peak current: 205 A
- Pulse width: 7.35 ms
- Wave form shape: Bi-polar trapezoid
- Peak dipole moment: 435,358 nIA
- Actual average EM Bird terrain clearance: 56 metres above the ground

Receiver

- X Coil diameter: 0.32 m
- Number of turns: 245
- Effective coil area: 19.69 m^2
- Z-Coil diameter: 1.2 m
- Number of turns: 100
- Effective coil area: 113.04 m^2

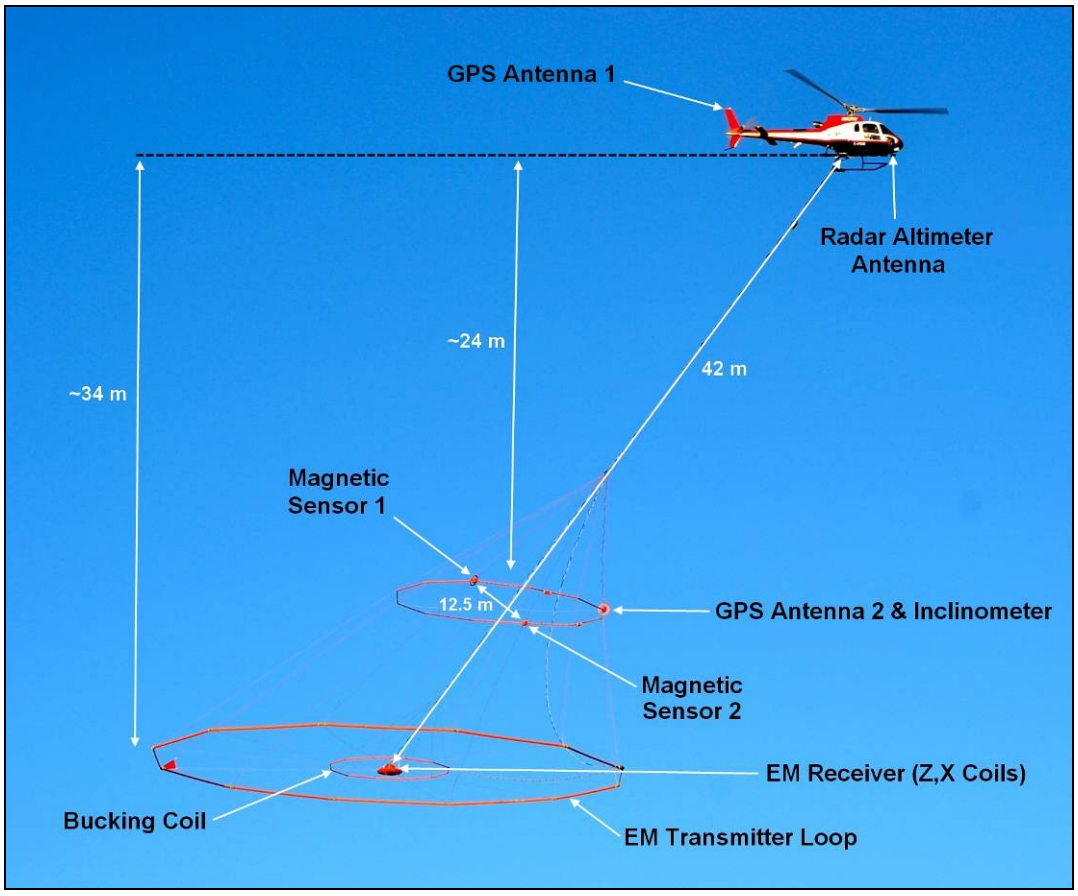

Figure 5: VTEM^{plus} System Configuration.

2.4.3 FULL WAVEFORM VTEM Sensor Calibration

The calibration is performed on the complete VTEM system installed in and connected to the helicopter, using special calibration equipment.

The procedure takes half-cycle files acquired and calculates a calibration file consisting of a single stacked half-cycle waveform. The purpose of the stacking is to attenuate natural and man-made magnetic signals, leaving only the response to the calibration signal.

2.4.4 Horizontal Magnetic Gradiometer

The horizontal magnetic gradiometer consists of two Geometrics split-beam field magnetic sensors with a sampling interval of 0.1 seconds. These sensors are mounted 12.5 metres apart on a separate loop, 10 metres above the EM bird. A GPS antenna and Gyro Inclinometer is installed on the separate loop to accurately record the tilt and position of the magnetic gradiomag bird.

2.4.5 Radar Altimeter

A Terra TRA 3000/TRI 40 radar altimeter was used to record terrain clearance. The antenna was mounted beneath the bubble of the helicopter cockpit (Figure 5).

2.4.6 GPS Navigation System

The navigation system used was a Geotech PC104 based navigation system utilizing a NovAtel's WAAS (Wide Area Augmentation System) enabled GPS receiver, Geotech navigate software, a full screen display with controls in front of the pilot to direct the flight and a NovAtel GPS antenna mounted on the helicopter tail (Figure 5). As many as 11 GPS and two WAAS satellites may be monitored at any one time. The positional accuracy or circular error probability (CEP) is 1.8 m, with WAAS active, it is 1.0 m. The co-ordinates of the block were set-up prior to the survey and the information was fed into the airborne navigation system. The second GPS antenna is installed on the additional magnetic loop together with Gyro Inclinometer.

2.4.7 Digital Acquisition System

A Geotech data acquisition system recorded the digital survey data on an internal compact flash card. Data is displayed on an LCD screen as traces to allow the operator to monitor the integrity of the system. The data type and sampling interval as provided in Table 4.

Table 4: Acquisition Sampling Rates

Data Type	Sampling
TDEM	0.1 sec
Magnetometer	0.1 sec
GPS Position	0.2 sec
Radar Altimeter	0.2 sec
Inclinometer	0.1 sec

2.5 Base Station

A combined magnetometer/GPS base station was utilized on this project. A Geometrics Cesium vapour magnetometer was used as a magnetic sensor with a sensitivity of 0.001 nT. The base station was recording the magnetic field together with the GPS time at 1 Hz on a base station computer.

The base station magnetometer sensor was installed in an open area (68º5'21.62 N, & 21º41'52.39 E); away from electric transmission lines and moving ferrous objects such as motor vehicles. The base station data were backed-up to the data processing computer at the end of each survey day.

3. PERSONNEL

The following Geotech Ltd. personnel were involved in the project.

Field:

Project Manager:	Jerome Vidal (Office)
Data QC:	Neil Fiset (Office)
Crew chief:	Sergio Martins
Operator:	Sergio Martins

The survey pilot and the mechanical engineer were employed directly by the helicopter operator – Air Walser.

Pilot:	Andrea Scadavino Emanuel Bertoldi
Mechanical Engineer:	Lorenzo Maciocu Nicola Viotti

Office:

Preliminary Data Processing:	Neil Fiset
Final Data Processing:	Shaolin Lu
Final Data QA/QC:	Alexander Prikhodko
Reporting/Mapping:	Wendy Acorn

Data acquisition phase was carried out under the supervision of Andrei Bagrianski, P. Geo, Chief Operating Officer. Processing and Interpretation phases were carried out under the supervision of Geoffrey Plastow, P. Geo, Data Processing Manager and Alexander Prikhodko P.Geo. PhD. Manager of Data Interpretation. The customer relations were looked after by Doug Pitcher.

4. DATA PROCESSING AND PRESENTATION

Data compilation and processing were carried out by the application of Geosoft OASIS Montaj and programs proprietary to Geotech Ltd.

4.1 Flight Path

The flight path, recorded by the acquisition program as WGS 84 latitude/longitude, was converted into the SWEREF99 Datum, SWEREF99 TM coordinate system in Oasis Montaj.

The flight path was drawn using linear interpolation between x, y positions from the navigation system. Positions are updated every second and expressed as UTM easting's (x) and UTM northing's (y).

4.2 Electromagnetic Data

The Full Waveform EM specific data processing operations included:

Half cycle stacking (performed at time of acquisition);
System response correction;
Parasitic and drift removal by deconvolution.

A three stage digital filtering process was used to reject major sferic events and to reduce noise levels. Local sferic activity can produce sharp, large amplitude events that cannot be removed by conventional filtering procedures. Smoothing or stacking will reduce their amplitude but leave a broader residual response that can be confused with geological phenomena. To avoid this possibility, a computer algorithm searches out and rejects the major sferic events.

The signal to noise ratio was further improved by the application of a low pass linear digital filter. This filter has zero phase shift which prevents any lag or peak displacement from occurring, and it suppresses only variations with a wavelength less than about 1 second or 15 metres. This filter is a symmetrical 1 sec linear filter.

The results are presented as stacked profiles of EM voltages for the time gates, in linear - logarithmic scale for the B-field Z component and dB/dt responses in the Z and X components. B-field Z component time channel recorded at 2.667 milliseconds after the termination of the impulse is also presented as a colour image. Calculated Time Constant (TAU) with anomaly contours of Calculated Vertical Derivative of TMI is presented in Appendix C and E. Resistivity Depth Image (RDI) is also presented in Appendix C and F.

VTEM has two receiver coil orientations. Z-axis coil is oriented parallel to the transmitter coil axis and both are horizontal to the ground. The X-axis coil is oriented parallel to the ground and along the line-of-flight. This combined two coil configuration provides information on the position, depth, dip and thickness of a conductor. Generalized modeling results of VTEM data, are shown in Appendix D.

In general X-component data produce cross-over type anomalies: from "+ to – "in flight direction of flight for "thin" sub vertical targets and from "- to +" in direction of flight for "thick" targets. Z component data produce double peak type anomalies for "thin" sub vertical targets and single peak for "thick" targets.

The limits and change-over of "thin-thick" depends on dimensions of a TEM system (Appendix D, Figure D-16).

Because of X component polarity is under line-of-flight, convolution Fraser Filter (Figure 6) is applied to X component data to represent axes of conductors in the form of grid map. In this case positive FF anomalies always correspond to "plus-to-minus" X data crossovers independent of the flight direction.

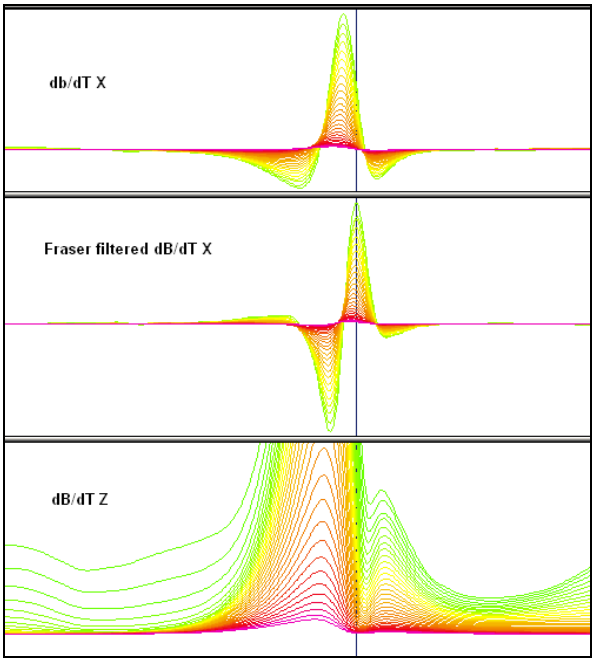

Figure 6: Z, X and Fraser filtered X (FFx) components for "thin" target.

4.3 Horizontal Magnetic Gradiometer Data

The horizontal gradients data from the VTEM^{plus} are measured by two magnetometers 12.5 m apart on an independent bird mounted10m above the VTEM loop. A GPS and a Gyro Inclinometer help to determine the positions and orientations of the magnetometers. The data from the two magnetometers are corrected for position and orientation variations, as well as for the diurnal variations using the base station data.

The position of the centre of the horizontal magnetic gradiometer bird is calculated form the GPS utilizing in-house processing tool in Geosoft. Following that total magnetic intensity is calculated at the center of the bird by calculating the mean values from both sensors. In addition to the total intensity advanced processing is done to calculate the in-line and cross-line (or lateral) horizontal gradient which enhance the understanding of magnetic targets. The in-line (longitudinal) horizontal gradient is calculated from the difference of two consecutive total magnetic field readings divided by the distance along the flight line direction, while the cross-line (lateral) horizontal magnetic gradient is calculated from the difference in the magnetic readings from both magnetic sensors divided by their horizontal separation.

Two advanced magnetic derivative products, the total horizontal derivative (THDR), and tilt angle derivative and are also created. The total horizontal derivative or gradient is also called the analytic signal, is defined as:

THDR = sqrt(Hx*Hx+Hy*Hy), where Hx and Hy are cross-line and in-line horizontal gradients.

The tilt angle derivative (TDR) is defined as:

TDR = arctan(Vz/THDR), where THDR is the total horizontal derivative, and Vz is the vertical derivative.

Measured cross-line gradients can help to enhance cross-line linear features during gridding.

5. DELIVERABLES

5.1 Survey Report

The survey report describes the data acquisition, processing, and final presentation of the survey results. The survey report is provided in two paper copies and digitally in PDF format.

5.2 Maps

Final maps were produced at scale of 1:50,000 for best representation of the survey size and line spacing. The coordinate/projection system used was SWEREF99 Datum, SWEREF99 TM. All maps show the flight path trace and topographic data; latitude and longitude are also noted on maps.

The preliminary and final results of the survey are presented as EM profiles, a late-time gate gridded EM channel, and a colour magnetic RTP TMI contour map. All Final maps have EM Anomaly picks. The following maps are presented on paper;

- VTEM dB/dt profiles Z Component, Time Gates 0.220 – 7.036 ms in linear – logarithmic scale.
- VTEM B-Field profiles Z Component, Time Gates 0.220 – 7.036 ms in linear – logarithmic scale.
- VTEM B-field late time Z Component colour image.
- VTEM dB/dt Calculated Time Constant (TAU) with contours of anomaly areas of the Calculated Vertical Derivative of TMI
- Fraser Filtered dB/dt X Component colour image
- Total magnetic intensity (TMI) colour image and contours.
- Magnetic Total Horizontal Gradient
- Magnetic Tilt-Angle Derivative

5.3 Digital Data

Two copies of the data and maps on DVD were prepared to accompany the report. Each DVD contains a digital file of the line data in GDB Geosoft Montaj format as well as the maps in Geosoft Montaj Map and PDF format.

- DVD structure.

  Data contains databases, grids and maps, as described below.
  Report contains a copy of the report and appendices in PDF format.

  Databases in Geosoft GDB format, containing the channels listed in Table 5.

Table 5: Geosoft GDB Data Format

Channel name	Units	Description
X_:	metres	UTM Easting SWEREF99 SWEREF99 TM
Y_:	metres	UTM Northing SWEREF99 SWEREF99 TM
Longitude:	Decimal Degrees	WGS 84 Longitude data
Latitude:	Decimal Degrees	WGS 84 Latitude data
Z:	metres	GPS antenna elevation (above Geoid)
Radar:	metres	helicopter terrain clearance from radar altimeter
Radarb:	metres	Calculated EM bird terrain clearance from radar altimeter
DEM:	metres	Digital Elevation Model
Gtime:	Seconds of the day	GPS time
Mag1L:	nT	Measured Total Magnetic field data (left sensor)
Mag1R:	nT	Measured Total Magnetic field data (right sensor)
Basemag:	nT	Magnetic diurnal variation data
Mag2LZ	nT	Z corrected (w.r.t. loop center) and diurnal corrected magnetic field left mag
Mag2RZ	nT	Z corrected (w.r.t. loop center) and diurnal corrected magnetic field right mag
TMI2	nT	Calculated from diurnal corrected total magnetic field intensity of the centre of the loop
TMI3	nT	Microleveled total magnetic field intensity of the centre of the loop
Hgcxline		measured cross-line gradient
Hginline		Calculated in-line gradient
CVG	nT/m	Calculated Magnetic Vertical Gradient
SFz[4]:	pV/(A*m^4)	Z dB/dt 0.021 millisecond time channel
SFz[5]:	pV/(A*m^4)	Z dB/dt 0.026 millisecond time channel
SFz[6]:	pV/(A*m^4)	Z dB/dt 0.031 millisecond time channel
SFz[7]:	pV/(A*m^4)	Z dB/dt 0.036 millisecond time channel
SFz[8]:	pV/(A*m^4)	Z dB/dt 0.042 millisecond time channel
SFz[9]:	pV/(A*m^4)	Z dB/dt 0.048 millisecond time channel
SFz[10]:	pV/(A*m^4)	Z dB/dt 0.055 millisecond time channel
SFz[11]:	pV/(A*m^4)	Z dB/dt 0.063 millisecond time channel
SFz[12]:	pV/(A*m^4)	Z dB/dt 0.073 millisecond time channel
SFz[13]:	pV/(A*m^4)	Z dB/dt 0.083 millisecond time channel
SFz[14]:	pV/(A*m^4)	Z dB/dt 0.096 millisecond time channel
SFz[15]:	pV/(A*m^4)	Z dB/dt 0.110 millisecond time channel
SFz[16]:	pV/(A*m^4)	Z dB/dt 0.126 millisecond time channel
SFz[17]:	pV/(A*m^4)	Z dB/dt 0.145 millisecond time channel
SFz[18]:	pV/(A*m^4)	Z dB/dt 0.167 millisecond time channel
SFz[19]:	pV/(A*m^4)	Z dB/dt 0.192 millisecond time channel
SFz[20]:	pV/(A*m^4)	Z dB/dt 0.220 millisecond time channel
SFz[21]:	pV/(A*m^4)	Z dB/dt 0.253 millisecond time channel
SFz[22]:	pV/(A*m^4)	Z dB/dt 0.290 millisecond time channel
SFz[23]:	pV/(A*m^4)	Z dB/dt 0.333 millisecond time channel
SFz[24]:	pV/(A*m^4)	Z dB/dt 0.383 millisecond time channel
SFz[25]:	pV/(A*m^4)	Z dB/dt 0.440 millisecond time channel
SFz[26]:	pV/(A*m^4)	Z dB/dt 0.505 millisecond time channel
SFz[27]:	pV/(A*m^4)	Z dB/dt 0.580 millisecond time channel
SFz[28]:	pV/(A*m^4)	Z dB/dt 0.667 millisecond time channel

Channel name	Units	Description
SFz[29]:	pV/(A*m^4)	Z dB/dt 0.766 millisecond time channel
SFz[30]:	pV/(A*m^4)	Z dB/dt 0.880 millisecond time channel
SFz[31]:	pV/(A*m^4)	Z dB/dt 1.010 millisecond time channel
SFz[32]:	pV/(A*m^4)	Z dB/dt 1.161 millisecond time channel
SFz[33]:	pV/(A*m^4)	Z dB/dt 1.333 millisecond time channel
SFz[34]:	pV/(A*m^4)	Z dB/dt 1.531 millisecond time channel
SFz[35]:	pV/(A*m^4)	Z dB/dt 1.760 millisecond time channel
SFz[36]:	pV/(A*m^4)	Z dB/dt 2.021 millisecond time channel
SFz[37]:	pV/(A*m^4)	Z dB/dt 2.323 millisecond time channel
SFz[38]:	pV/(A*m^4)	Z dB/dt 2.667 millisecond time channel
SFz[39]:	pV/(A*m^4)	Z dB/dt 3.063 millisecond time channel
SFz[40]:	pV/(A*m^4)	Z dB/dt 3.521 millisecond time channel
SFz[41]:	pV/(A*m^4)	Z dB/dt 4.042 millisecond time channel
SFz[42]:	pV/(A*m^4)	Z dB/dt 4.641 millisecond time channel
SFz[43]:	pV/(A*m^4)	Z dB/dt 5.333 millisecond time channel
SFz[44]:	pV/(A*m^4)	Z dB/dt 6.125 millisecond time channel
SFz[45]:	pV/(A*m^4)	Z dB/dt 7.036 millisecond time channel
SFz[46]:	pV/(A*m^4)	Z dB/dt 8.083 millisecond time channel
SFz[47]:	pV/(A*m^4)	Z dB/dt 9.286 millisecond time channel
SFz[48]:	pV/(A*m^4)	Z dB/dt 10.667 millisecond time channel
SFx[20]:	pV/(A*m^4)	X dB/dt 0.220 millisecond time channel
SFx[21]:	pV/(A*m^4)	X dB/dt 0.253 millisecond time channel
SFx[22]:	pV/(A*m^4)	X dB/dt 0.290 millisecond time channel
SFx[23]:	pV/(A*m^4)	X dB/dt 0.333 millisecond time channel
SFx[24]:	pV/(A*m^4)	X dB/dt 0.383 millisecond time channel
SFx[25]:	pV/(A*m^4)	X dB/dt 0.440 millisecond time channel
SFx[26]:	pV/(A*m^4)	X dB/dt 0.505 millisecond time channel
SFx[27]:	pV/(A*m^4)	X dB/dt 0.580 millisecond time channel
SFx[28]:	pV/(A*m^4)	X dB/dt 0.667 millisecond time channel
SFx[29]:	pV/(A*m^4)	X dB/dt 0.766 millisecond time channel
SFx[30]:	pV/(A*m^4)	X dB/dt 0.880 millisecond time channel
SFx[31]:	pV/(A*m^4)	X dB/dt 1.010 millisecond time channel
SFx[32]:	pV/(A*m^4)	X dB/dt 1.161 millisecond time channel
SFx[33]:	pV/(A*m^4)	X dB/dt 1.333 millisecond time channel
SFx[34]:	pV/(A*m^4)	X dB/dt 1.531 millisecond time channel
SFx[35]:	pV/(A*m^4)	X dB/dt 1.760 millisecond time channel
SFx[36]:	pV/(A*m^4)	X dB/dt 2.021 millisecond time channel
SFx[37]:	pV/(A*m^4)	X dB/dt 2.323 millisecond time channel
SFx[38]:	pV/(A*m^4)	X dB/dt 2.667 millisecond time channel
SFx[39]:	pV/(A*m^4)	X dB/dt 3.063 millisecond time channel
SFx[40]:	pV/(A*m^4)	X dB/dt 3.521 millisecond time channel
SFx[41]:	pV/(A*m^4)	X dB/dt 4.042 millisecond time channel
SFx[42]:	pV/(A*m^4)	X dB/dt 4.641 millisecond time channel
SFx[43]:	pV/(A*m^4)	X dB/dt 5.333 millisecond time channel
SFx[44]:	pV/(A*m^4)	X dB/dt 6.125 millisecond time channel
SFx[45]:	pV/(A*m^4)	X dB/dt 7.036 millisecond time channel
SFx[46]:	pV/(A*m^4)	X dB/dt 8.083 millisecond time channel
SFx[47]:	pV/(A*m^4)	X dB/dt 9.286 millisecond time channel
SFx[48]:	pV/(A*m^4)	X dB/dt 10.667 millisecond time channel
BFz	(pV*ms)/(A*m^4)	Z B-Field data for time channels 4 to 48

Channel name	Units	Description
BFx	(pV*ms)/(A*m^4)	X B-Field data for time channels 20 to 48
SFxFF	pV/(A*m^4)	Fraser Filtered X dB/dt
TauSF	ms	Time constant dB/dt
NchanSF		Latest time channels of TAU calculation
TauBF	ms	Time constant B-Field
NchanBF		Latest time channels of TAU calculation
PLM:		50 Hz power line monitor

Electromagnetic B-field and dB/dt Z component data is found in array channel format between indexes 4 – 48, and X component data from 20 – 48, as described above.

- Database of the Resistivity Depth Images in Geosoft GDB format, containing the following channels:

Table 6: Geosoft Resistivity Depth Image GDB Data Format

Channel name	Units	Description
Xg:	metres	UTM Easting SWEREF99 SWEREF99 TM
Yg:	metres	UTM Northing SWEREF99 SWEREF99 TM
Dist:	meters	Distance from the beginning of the line
Depth:	meters	array channel, depth from the surface
Z:	meters	array channel, depth from sea level
AppRes:	Ohm-m	array channel, Apparent Resistivity
TR:	meters	EM system height from sea level
Topo:	meters	digital elevation model
Radarb:	metres	Calculated EM bird terrain clearance from radar altimeter
SF:	pV/(A*m^4)	array channel, dB/dT
MAG:	nT	TMI data
CVG:	nT/m	CVG data
DOI:	metres	Depth of Investigation: a measure of VTEM depth effectiveness
PLM:		60Hz Power Line Monitor

- Database of the VTEM Waveform “AB1374_waveform_final.gdb” in Geosoft GDB format, containing the following channels:

  Time: Sampling rate interval, 5.2083 milliseconds
  Tx_Current: Output current of the transmitter (Amp)

- Grids in Geosoft GRD and GeoTIFF format, as follows:

  BFz38: B-Field Z Component Channel 38 (Time Gate 2.667 ms)
  TMI: Total Magentic Intensity (TMI)
  CVG: Calculated Magnetic Vertical Gradient of TMI (nT/m)
  DEM: Digital Elevation Model (metres)
  PLM: Power Line Monitor
  Hgcxline: Measured Cross-Line Gradient (nT/m)
  Hginline: Measured In-Line Gradient (nT/m)
  SFxFF23: Fraser Filtered dB/dt X Component Channel 23 (time Gate 0.333 ms)
  SFz7: dB/dt Z Component Channel 7 (Time Gate 0.036 ms)
  SFz26: dB/dt Z Component Channel 26 (Time Gate 0.505 ms)
  SFz45: dB/dt Z Component Channel 45 (Time Gate 7.036 ms)

TauBF:	B-Field Z Component, Calculated Time Constant (ms)
TauSF:	dB/dt Z Component, Calculated Time Constant (ms)
TotHGrad:	Magnetic Total Horizontal Gradient (nT/m)
Tiltdrv:	Magnetic Tilt derivative (radians)

A Geosoft .GRD file has a .GI metadata file associated with it, containing grid projection information. A grid cell size of 125 metres was used.

- Maps at 1:50,000 in Geosoft MAP format, as follows:

AB1374_50k_dBdt:	dB/dt profiles Z Component, Time Gates 0.220 – 7.036 ms in linear – logarithmic scale.
AB1374_50k_Bfield:	B-field profiles Z Component, Time Gates 0.220 – 7.036 ms in linear – logarithmic scale.
AB1374_50k_BFz38:	B-field Z Component Channel 38, Time Gate 2.667 ms colour image.
AB1374_50k_TMI:	Total magnetic intensity (TMI) colour image and contours.
AB1374_50k_TauSF:	dB/dt Calculated Time Constant (Tau) with contours of anomaly areas of the Calculated Vertical Derivative of TMI
AB1374_50k_SFxFF23:	Fraser Filtered dB/dt X Component Channel 23, Time Gate 0.333 ms colour image.
AB1374_50k_TotHGrad:	Magnetic Total Horizontal Gradient colour image.
AB1374_50k_TiltDrv:	Magnetic Tilt-Angle Derivative colour image.

Maps are also presented in PDF format.

- 1:50,000 topographic vectors were taken from the NRCAN Geogratis database at; http://geogratis.gc.ca/geogratis/en/index.html.

- A Google Earth file *AB1374_SGU.kml* showing the flight path of the block is included. Free versions of Google Earth software from: http://earth.google.com/download-earth.html

6. CONCLUSIONS AND RECOMMENDATIONS

A helicopter-borne versatile time domain electromagnetic (VTEM) geophysical survey has been completed over the Barents-Lainio TEM block situated near KIruna, Sweden.

The total area coverage is 2088 km^2. Total survey line coverage is 4531 line kilometres. The principal sensors included a Time Domain EM system and horizontal magnetic gradiometer using two cesium magnetometers. Results have been presented as stacked profiles, and contour colour images at a scale of 1:50,000. A formal Interpretation has not been included or requested.

Based on the geophysical results obtained, a number of TEM anomalous zones are identified across the property. They can be seen overlapping the TAU decay parameter image presented with the calculated vertical magnetic gradient (CVG) contours (see Appendix C).

The major and strong anomalous zones are on the western (between T1810 and T1860) and eastern (T1920 and T1970) parts of the block. The anomalous zones are strongly associated with trends reflected in magnetic field. The conductors induced the strong anomalies are considered as “thin” and “thick” targets in many cases clearly steeply dipping.

Comparatively weak linear anomalous zone crosses the block in the central part in SW-NE direction along a dyke similar magnetic anomaly. The source of the anomalous zone is considered as a lithological or an alteration zone.

According to apparent resistivity depth images over selected lines (see Appendix C), the estimated depths to the top of potential targets is beginning from around 50 meters. The L1130, L1450, L1560 RDI sections represent the eastern strong anomalous zone and part of the central weak anomalous zone. The L1451 and L1561 RDI sections represents western anomalous zone partly the central weak anomalous zone.

In addition, several local anomalous zones of interests are detected across the property. The local anomalies can be seen at around T1960 between L1450 and L1490. The estimated depth from the surface to the top of the potential conductor is up to 450m (reference on RDI_L1450 in *Appendix C*).

There is a major power line going through the eastern part of the property (see power line image below) and nearby anomalous zones might be interfered. On the other hand, some of anomalous zones probably correspond to ground sources (water bodies, etc.); therefore, all anomalous zones which are related to ground sources and nearby to power lines must be investigated.

If the conductors correspond to an exploration model on the area it is recommended picking EM anomalies with conductance grading and center localization of the targets, detail resistivity depth imaging and plate modeling with test drill hole parameters planning prior to ground follow up and drill testing. Since most of conductive zones are associated with magnetic anomalies, attendant inversion/modeling of magnetic field is also recommended.

Respectfully submitted[2],

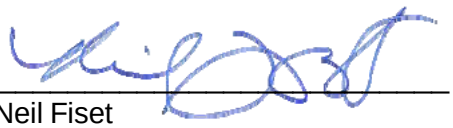

Neil Fiset
Geotech Ltd.

Shaolin Lu
Geotech Ltd

Geoffrey Plastow, P. Geo
Data Processing Manager
Geotech Ltd.

November, 2013

[2] Final data processing of the EM and magnetic data were carried out by Neil Fiset and Shaolin Lu, from the office of Geotech Ltd. in Aurora, Ontario, under the supervision of Geoffrey Plastow, P.Geo., Data Processing Manager.

APPENDIX A

SURVEY BLOCK LOCATION MAP

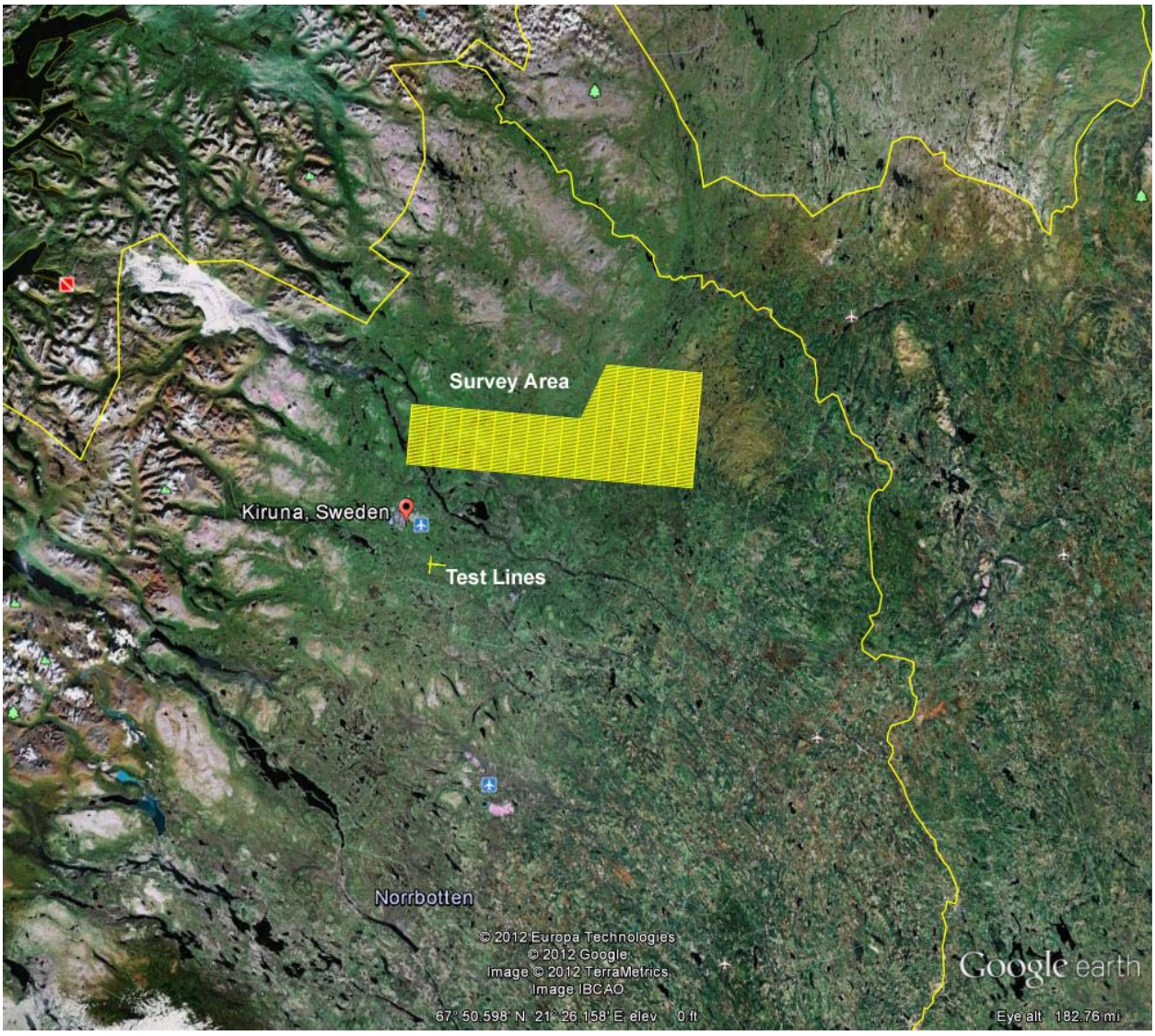

Survey Overview of the Survey Area

APPENDIX B

SURVEY BLOCK COORDINATES

(WGS 84, UTM Zone 34 North)

X	Y
469100.1	7558820.9
519248	7555092.1
526763.4	7570675.2
555128.8	7568280
552243.4	7533647.2
467631.2	7540776.5

APPENDIX C

GEOPHYSICAL MAPS[1]

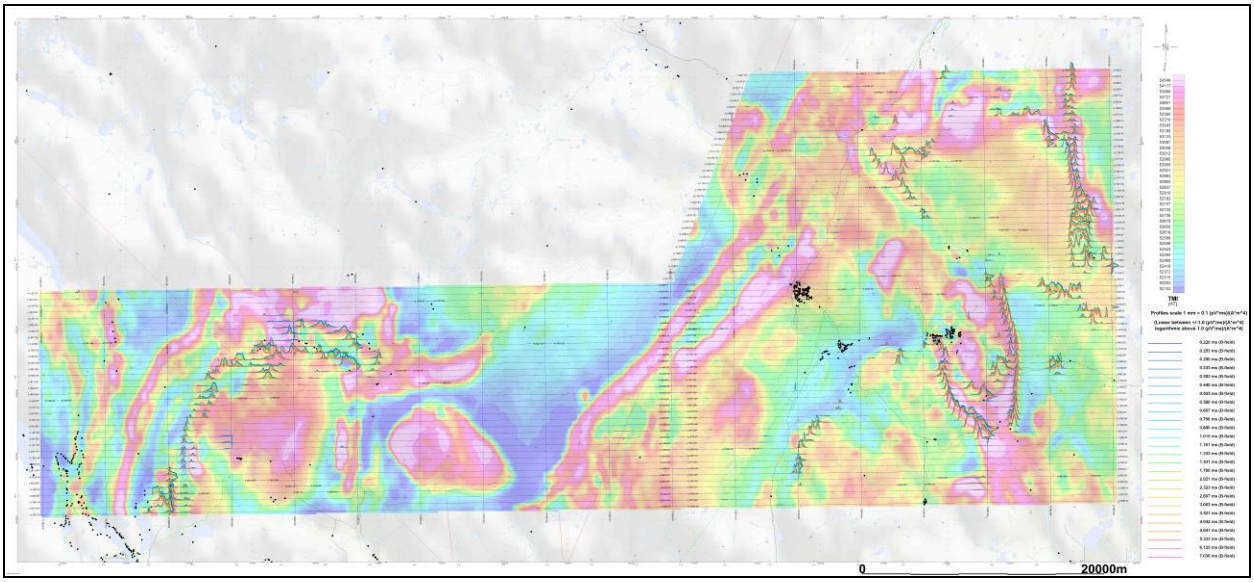

VTEM B-Field Z Component Profiles, Time Gates 0.220 to 7.036 ms

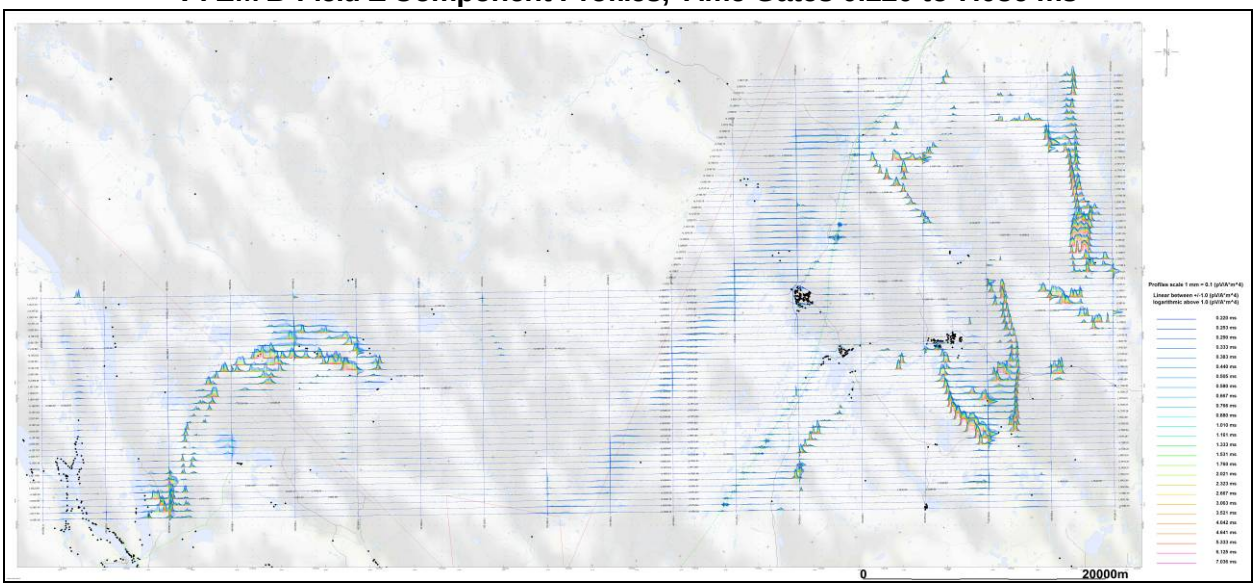

VTEM dB/dt Z Component Profiles, Time Gates 0.220 to 7.036 ms

[1] Full size geophysical maps are also available in PDF format on the final DVD

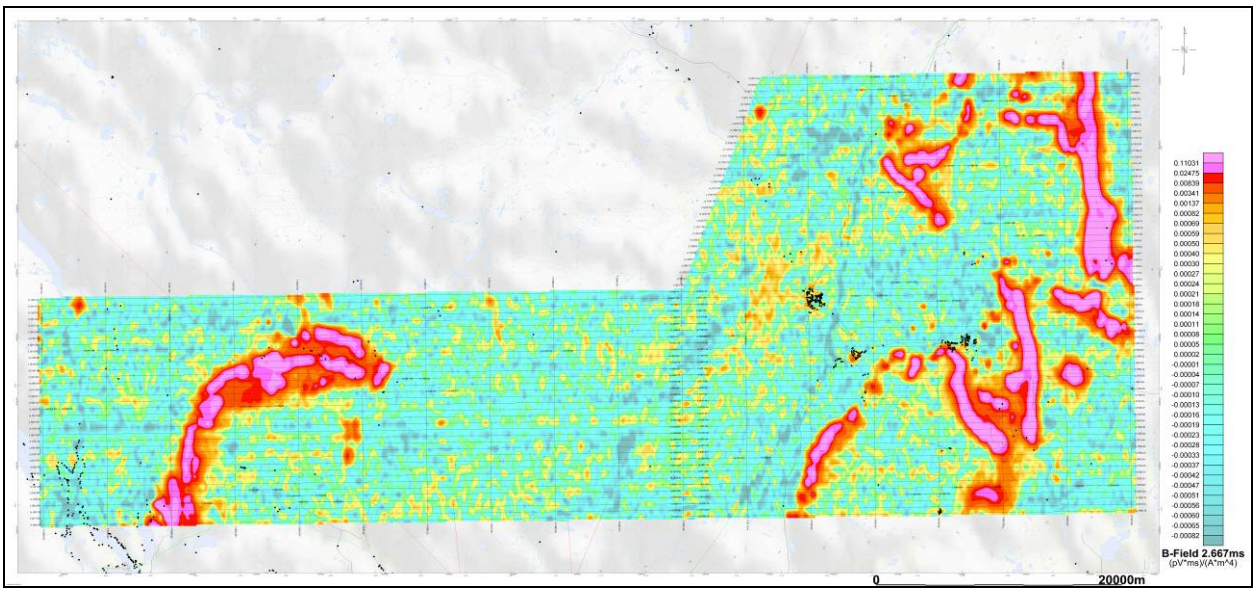

VTEM B-Field Z Component Channel 38, Time Gate 2.667 ms

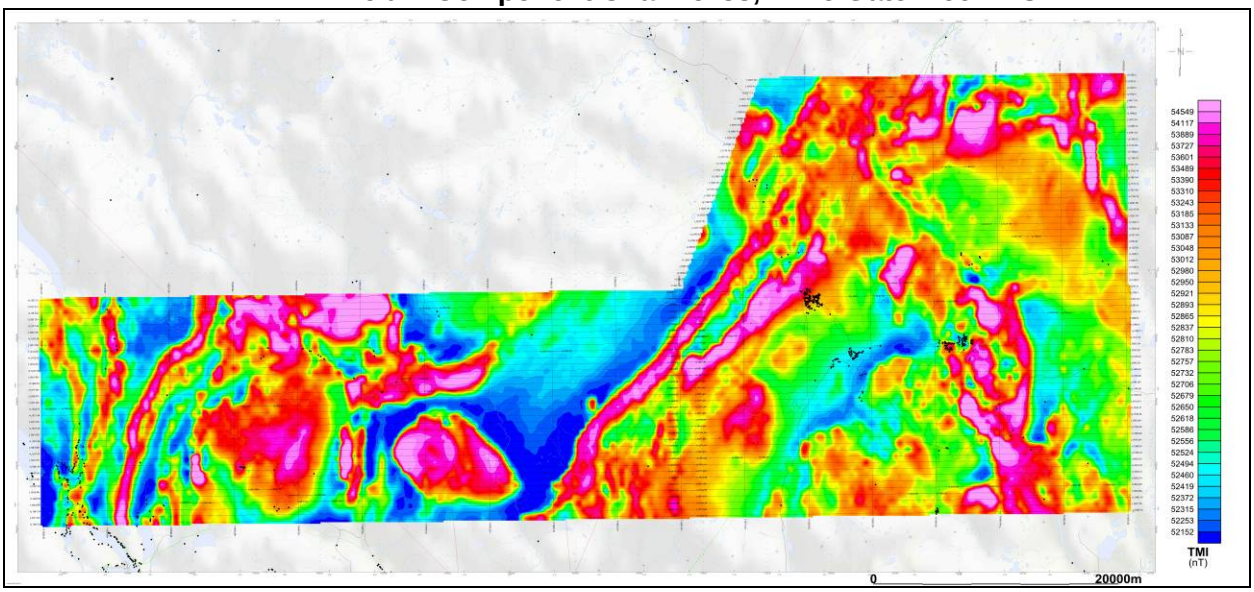

Total Magnetic Intensity (TMI)

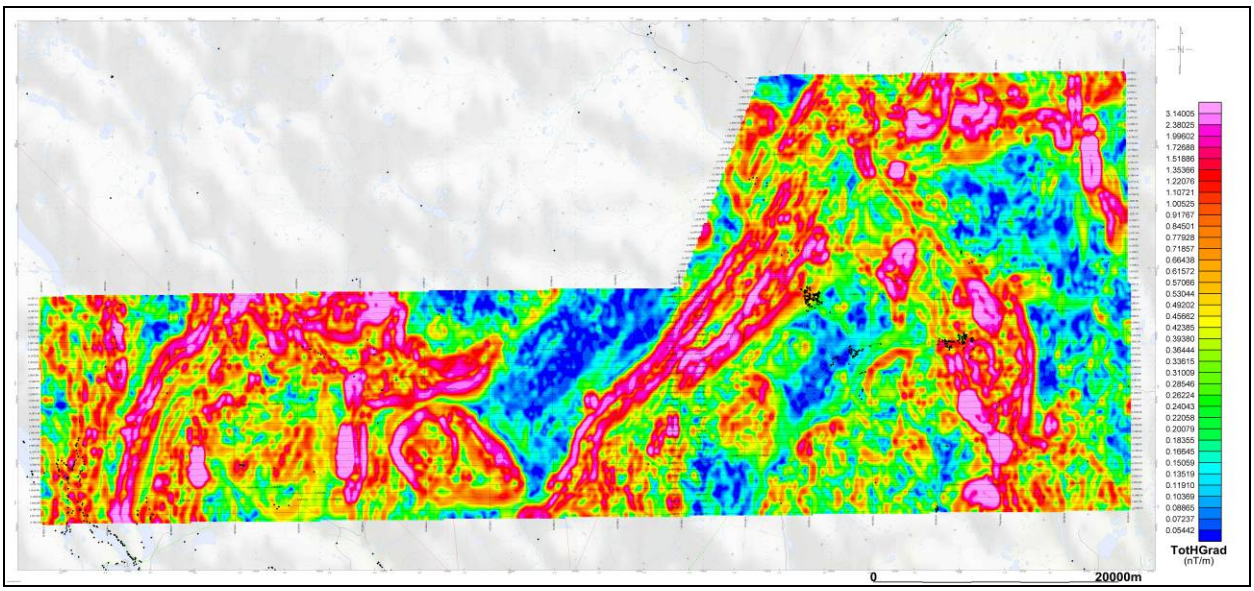

Magnetic Total Horizontal Gradient

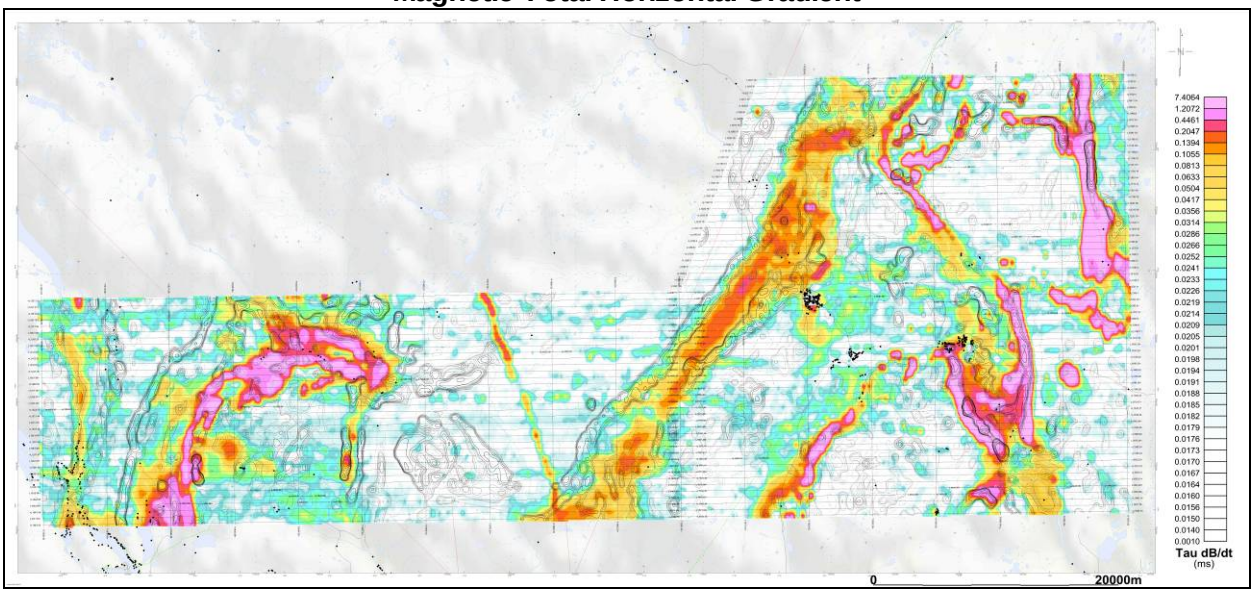

dB/dt Calculated Time Constant (Tau) with contours of anomaly areas of the Calculated Vertical Derivative of TMI

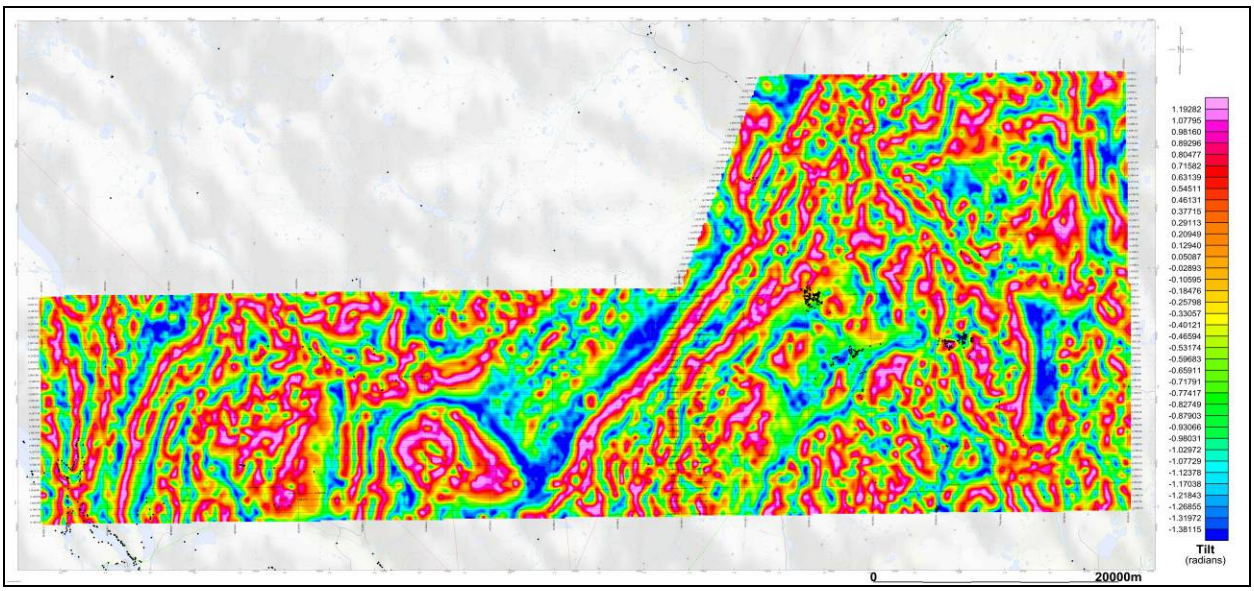

Magnetic Tilt – Angle Derivative

RESISTIVITY DEPTH IMAGE (RDI) MAPS

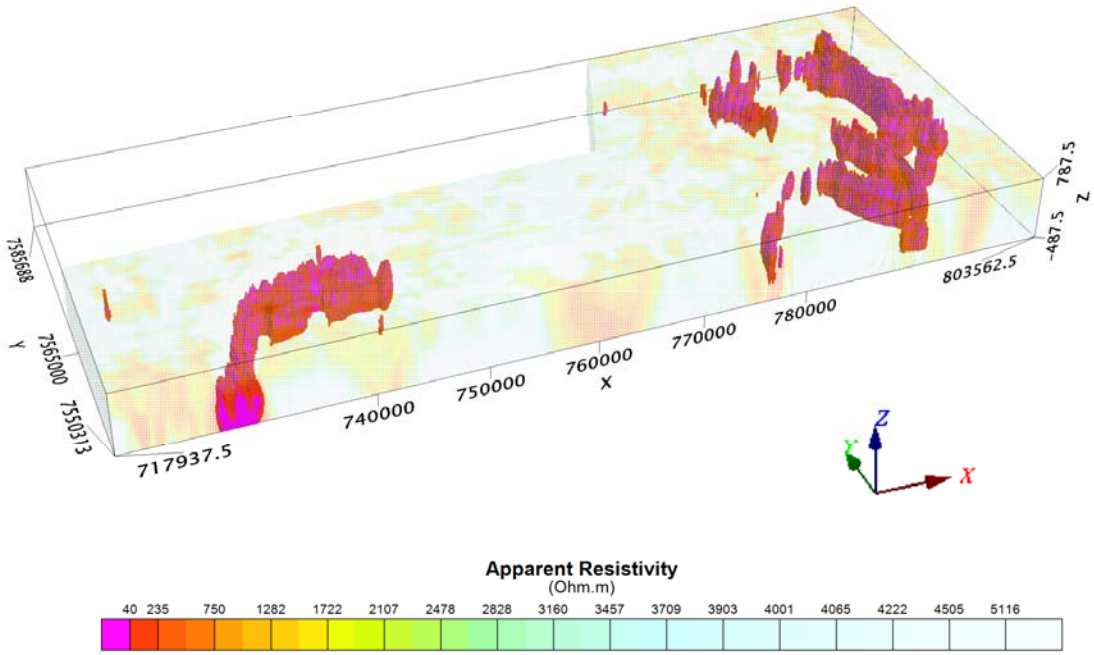

3D Resistivity-Depth Image (RDI)

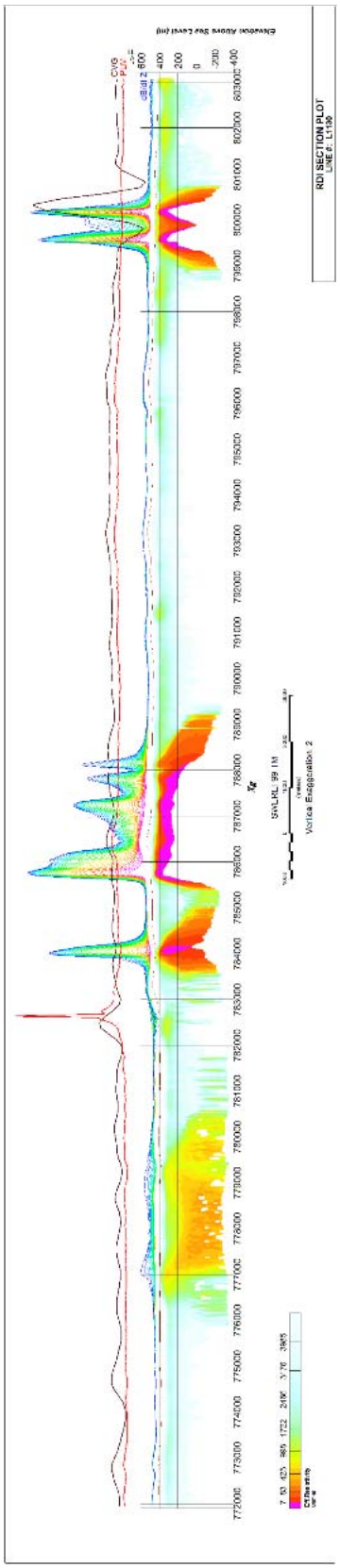

Line 1130

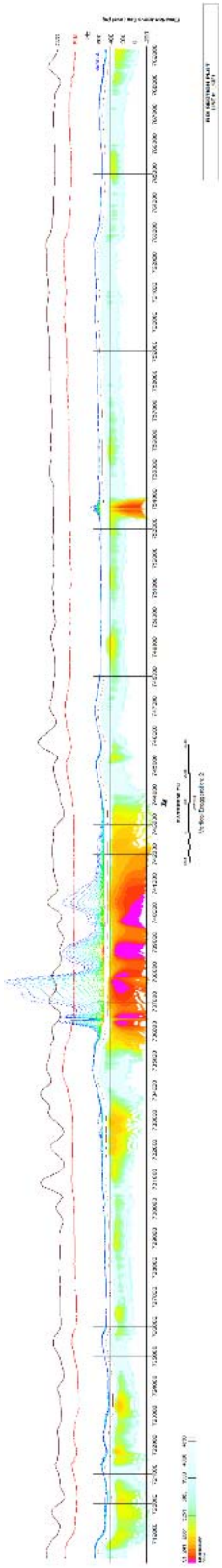

Line 1381

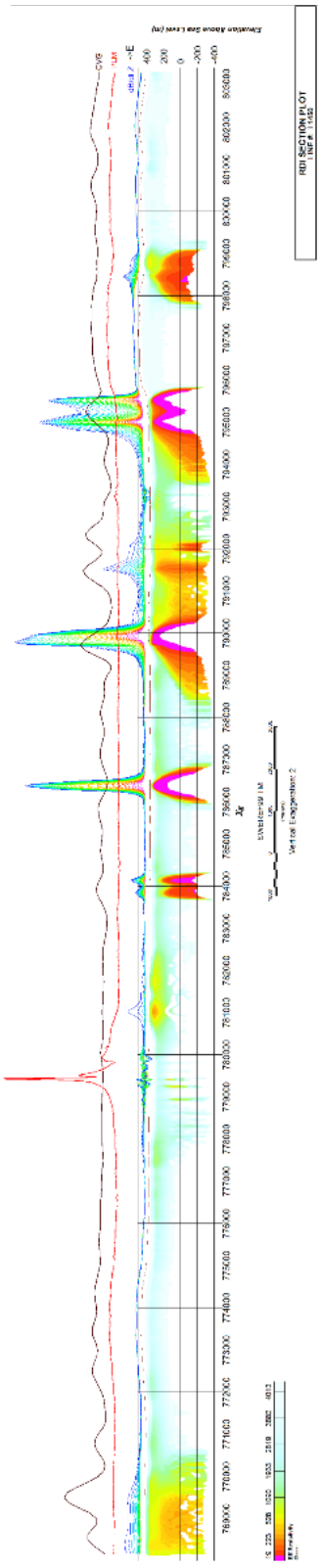

Line 1450

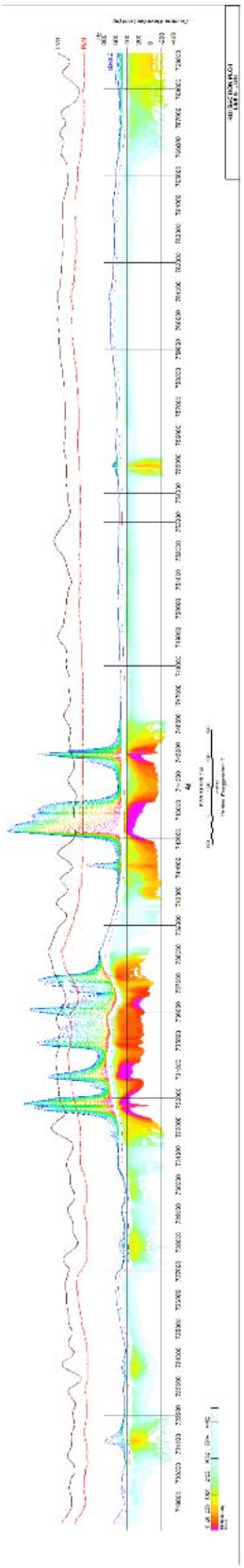

Line 1451

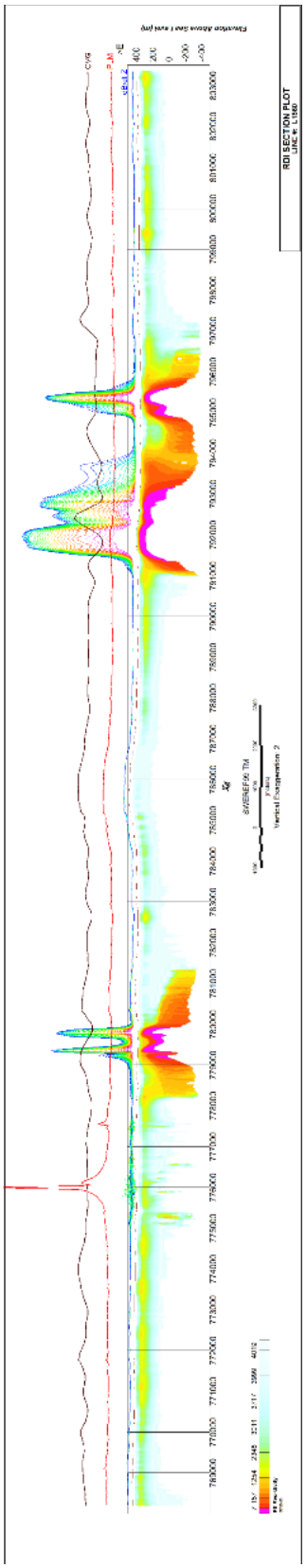

Line 1560

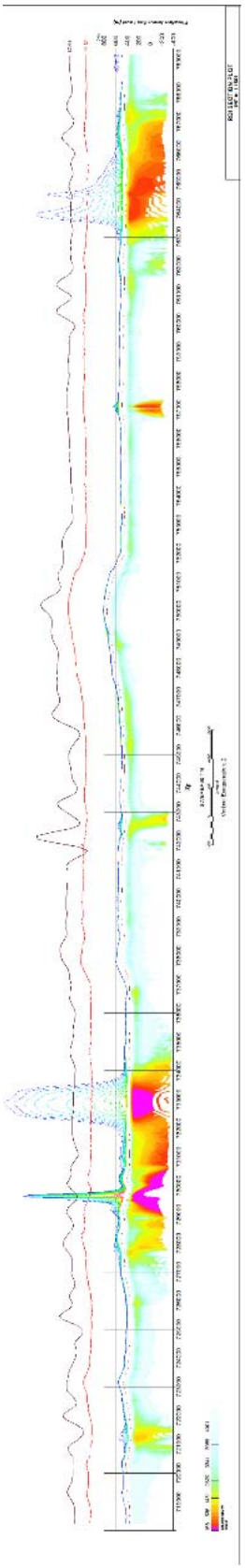

Line 1561

APPENDIX D

GENERALIZED MODELING RESULTS OF THE VTEM SYSTEM

Introduction

The VTEM system is based on a concentric or central loop design, whereby, the receiver is positioned at the centre of a transmitter loop that produces a primary field. The wave form is a bi-polar, modified square wave with a turn-on and turn-off at each end.

During turn-on and turn-off, a time varying field is produced (dB/dt) and an electro-motive force (emf) is created as a finite impulse response. A current ring around the transmitter loop moves outward and downward as time progresses. When conductive rocks and mineralization are encountered, a secondary field is created by mutual induction and measured by the receiver at the centre of the transmitter loop.

Efficient modeling of the results can be carried out on regularly shaped geometries, thus yielding close approximations to the parameters of the measured targets. The following is a description of a series of common models made for the purpose of promoting a general understanding of the measured results.

A set of models has been produced for the Geotech VTEM® system dB/dT Z and X components (see models D1 to D15). The Maxwell ™ modeling program (EMIT Technology Pty. Ltd. Midland, WA, AU) used to generate the following responses assumes a resistive half-space. The reader is encouraged to review these models, so as to get a general understanding of the responses as they apply to survey results. While these models do not begin to cover all possibilities, they give a general perspective on the simple and most commonly encountered anomalies.

As the plate dips and departs from the vertical position, the peaks become asymmetrical.

As the dip increases, the aspect ratio (Min/Max) decreases and this aspect ratio can be used as an empirical guide to dip angles from near 90º to about 30º. The method is not sensitive enough where dips are less than about 30º.

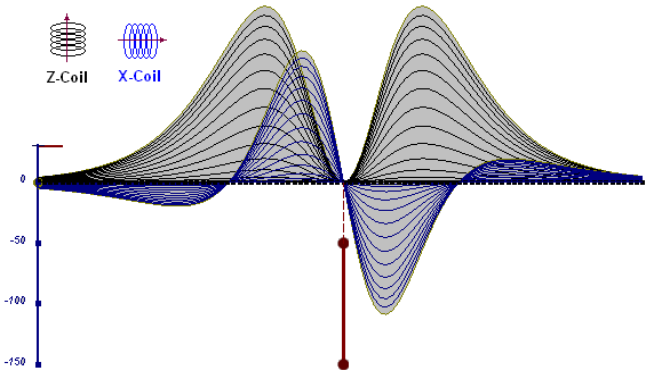

Figure D-1: vertical thin plate

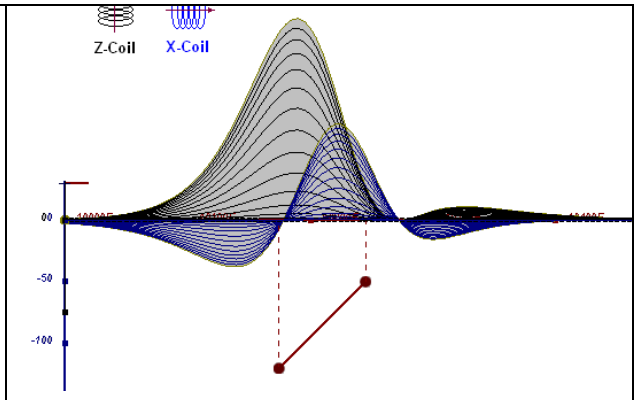

Figure D-2: inclined thin plate

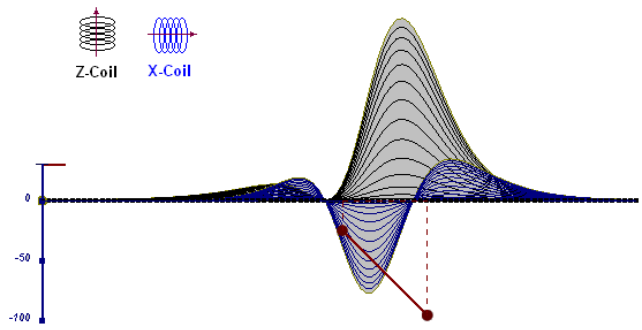

Figure D-3: inclined thin plate

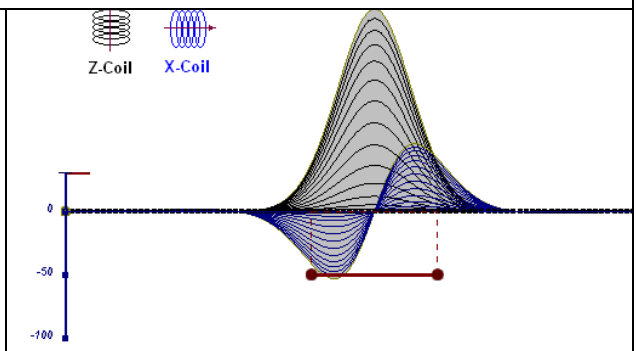

Figure D-4: horizontal thin plate

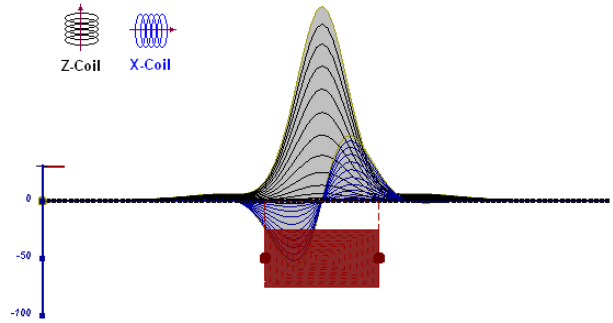

Figure D-5: horizontal thick plate (linear scale of the response)

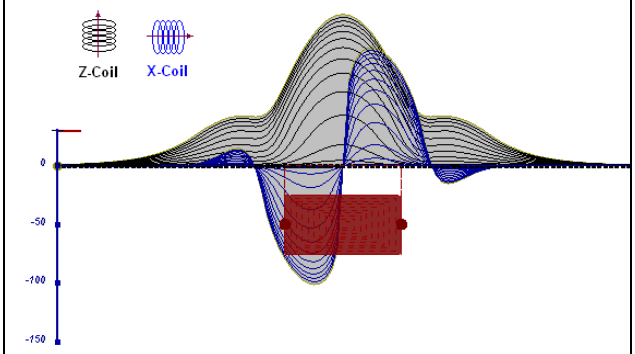

Figure D-6: horizontal thick plate (log scale of the response)

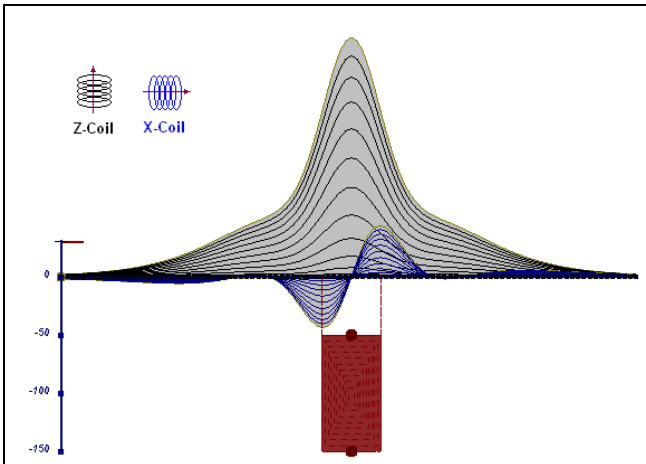

Figure D-7: vertical thick plate (linear scale of the response). 50 m depth

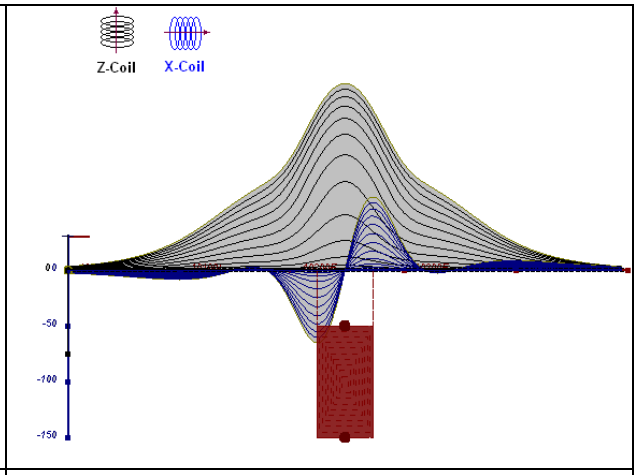

Figure D-8: vertical thick plate (log scale of the response). 50 m depth

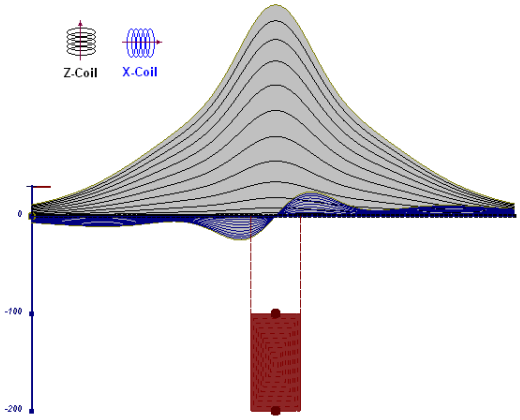

Figure D-9: vertical thick plate (linear scale of the response). 100 m depth

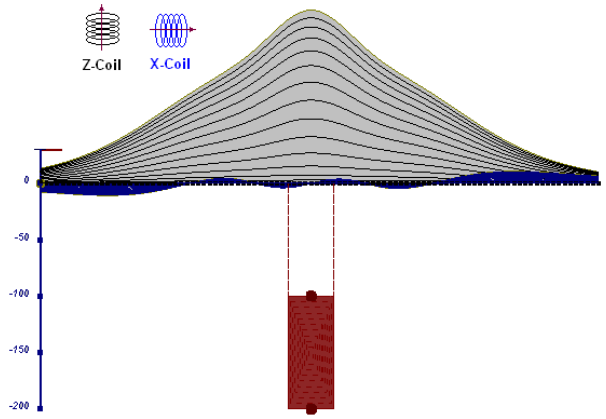

Figure D-10: vertical thick plate (linear scale of the response). Depth/hor.thickness=2.5

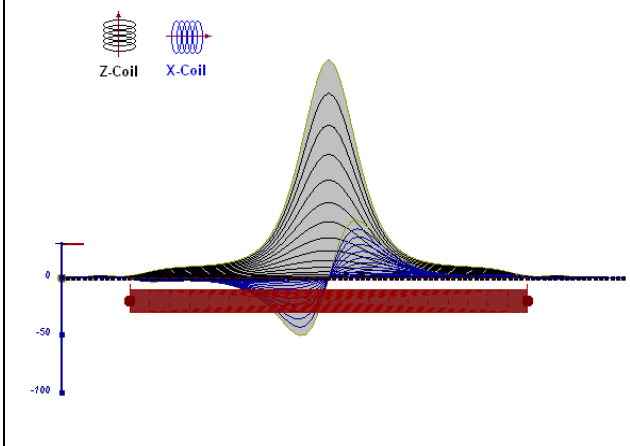

Figure D-10: horizontal thick plate (linear scale of the response)

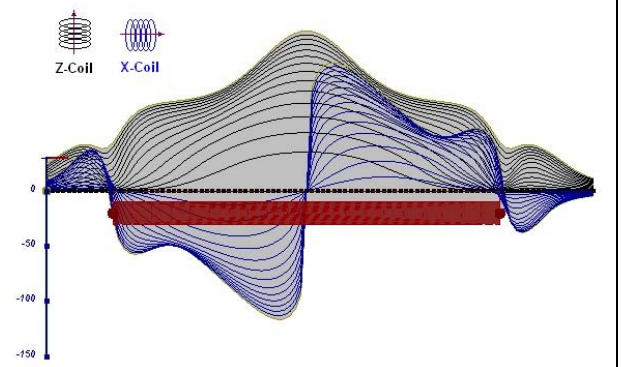

Figure D-11: horizontal thick plate (log scale of the response)

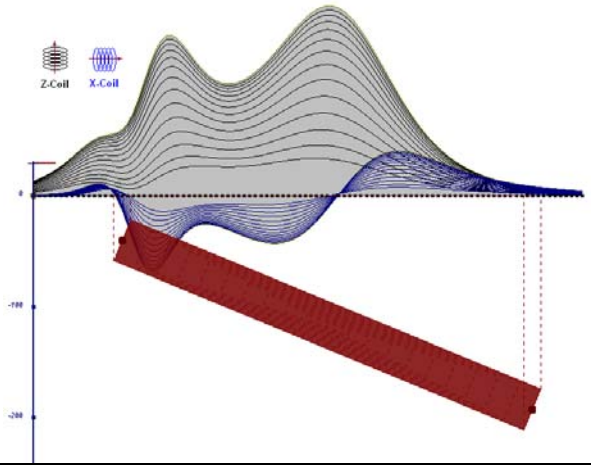

Figure D-12: inclined long thick plate

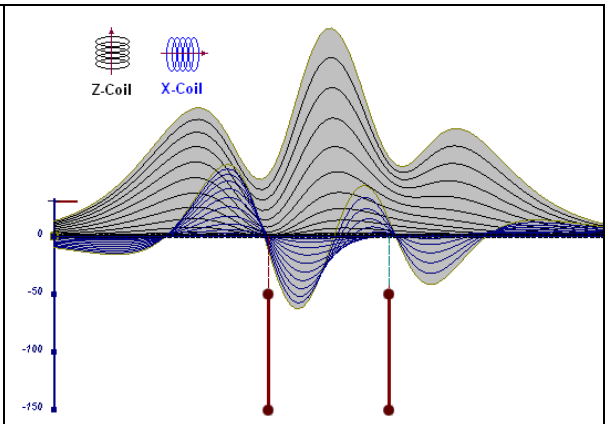

Figure D-13: two vertical thin plates

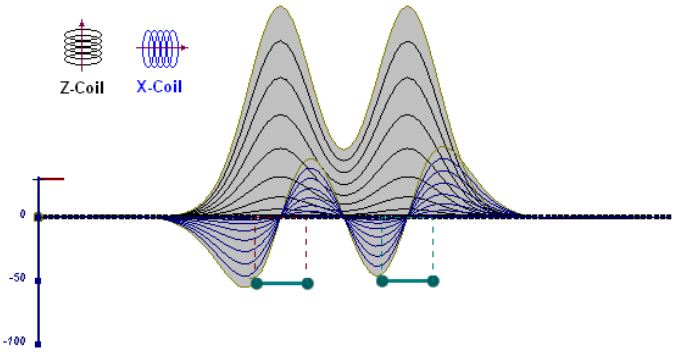

Figure D-14: two horizontal thin plates

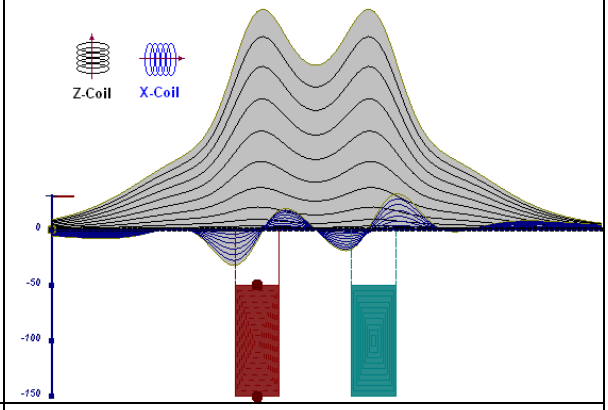

Figure D-15: two vertical thick plates

The same type of target but with different thickness, for example, creates different form of the response:

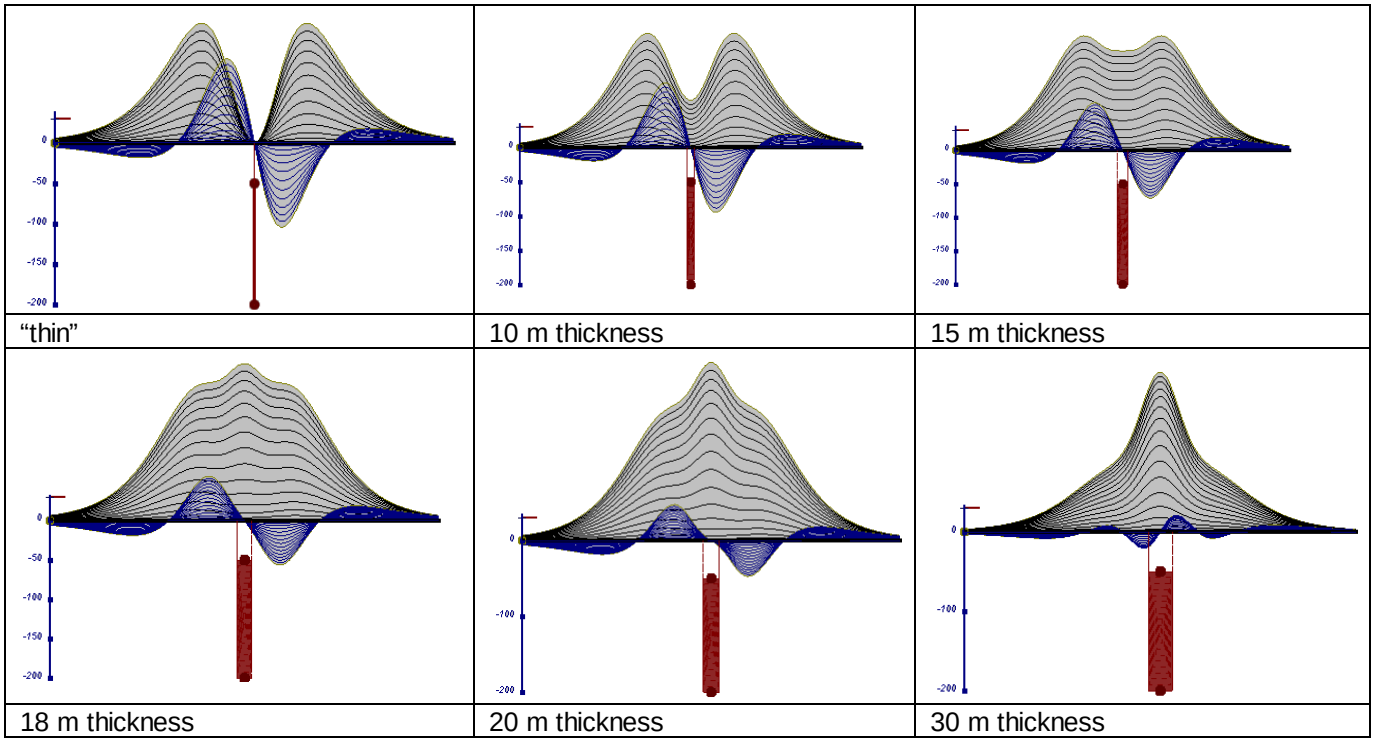

Figure D-16: Conductive vertical plate, depth 50 m, strike length 200 m, depth extends 150 m.

Alexander Prikhodko, PhD, P.Geo
Geotech Ltd.

September 2010

APPENDIX E

EM TIME CONSTANT (TAU) ANALYSIS

Estimation of time constant parameter[1] in transient electromagnetic method is one of the steps toward the extraction of the information about conductances beneath the surface from TEM measurements.

The most reliable method to discriminate or rank conductors from overburden, background or one and other is by calculating the EM field decay time constant (TAU parameter), which directly depends on conductance despite their depth and accordingly amplitude of the response.

Theory

As established in electromagnetic theory, the magnitude of the electro-motive force (emf) induced is proportional to the time rate of change of primary magnetic field at the conductor. This emf causes eddy currents to flow in the conductor with a characteristic transient decay, whose Time Constant (Tau) is a function of the conductance of the survey target or conductivity and geometry (including dimensions) of the target. The decaying currents generate a proportional secondary magnetic field, the time rate of change of which is measured by the receiver coil as induced voltage during the Off time.

The receiver coil output voltage ($\mathbf{e_0}$) is proportional to the time rate of change of the secondary magnetic field and has the form,

$$e_0 \alpha (1 / \tau) e^{-(t/\tau)}$$

Where,
τ = L/R is the characteristic time constant of the target (TAU)
R = resistance
L = inductance

From the expression, conductive targets that have small value of resistance and hence large value of τ yield signals with small initial amplitude that decays relatively slowly with progress of time. Conversely, signals from poorly conducting targets that have large resistance value and smallτ, have high initial amplitude but decay rapidly with time[1] (Fig. E1).

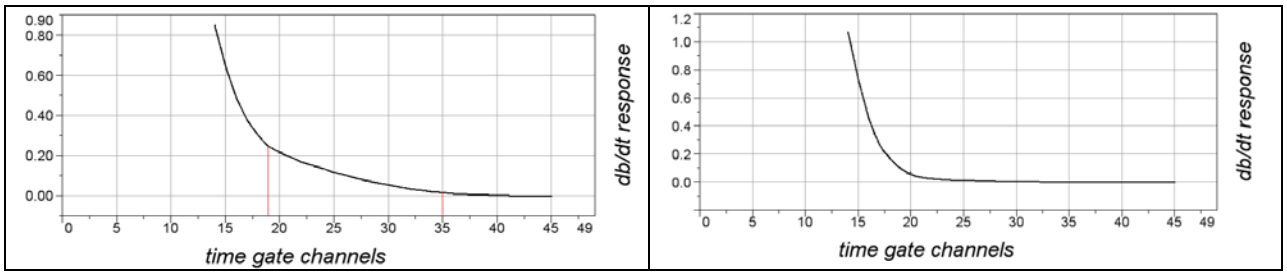

Figure E-1: Left – presence of good conductor, right – poor conductor.

[1] McNeill, JD, 1980, "Applications of Transient Electromagnetic Techniques", Technical Note TN-7 page 5, Geonics Limited, Mississauga, Ontario.

EM Time Constant (Tau) Calculation

The EM Time-Constant (TAU) is a general measure of the speed of decay of the electromagnetic response and indicates the presence of eddy currents in conductive sources as well as reflecting the "conductance quality" of a source. Although TAU can be calculated using either the measured dB/dt decay or the calculated B-field decay, dB/dt is commonly preferred due to better stability (S/N) relating to signal noise. Generally, TAU calculated on base of early time response reflects both near surface overburden and poor conductors whereas, in the late ranges of time, deep and more conductive sources, respectively. For example early time TAU distribution in an area that indicates conductive overburden is shown in Figure 2.

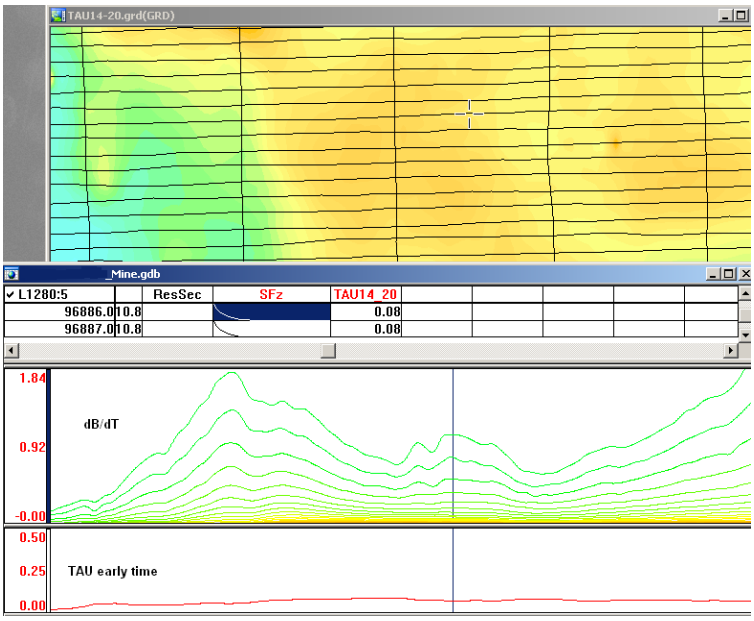

Figure E-2: Map of early time TAU. Area with overburden conductive layer and local sources.

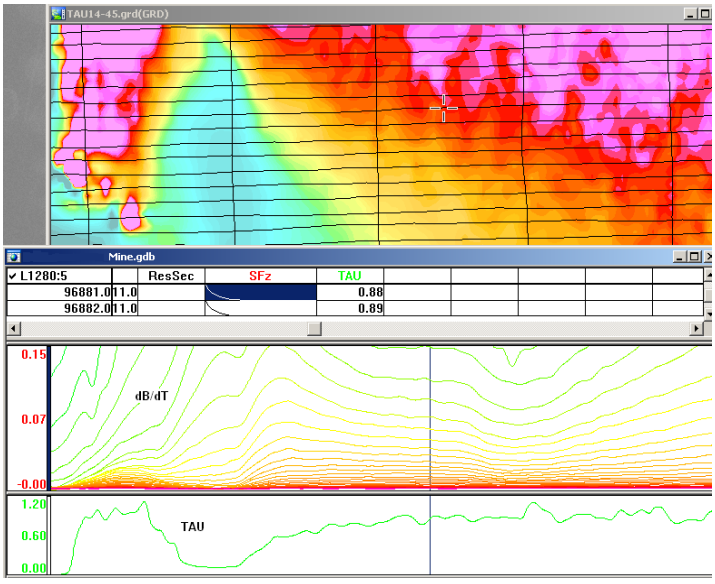

Figure E-3: Map of full time range TAU with EM anomaly due to deep highly conductive target.

There are many advantages of TAU maps:

- TAU depends only on one parameter (conductance) in contrast to response magnitude;
- TAU is integral parameter, which covers time range and all conductive zones and targets are displayed independently of their depth and conductivity on a single map.
- Very good differential resolution in complex conductive places with many sources with different conductivity.
- Signs of the presence of good conductive targets are amplified and emphasized independently of their depth and level of response accordingly.

In the example shown in Figure 4 and 5, three local targets are defined, each of them with a different depth of burial, as indicated on the resistivity depth image (RDI). All are very good conductors but the deeper target (number 2) has a relatively weak dB/dt signal yet also features the strongest total TAU (Figure 4). This example highlights the benefit of TAU analysis in terms of an additional target discrimination tool.

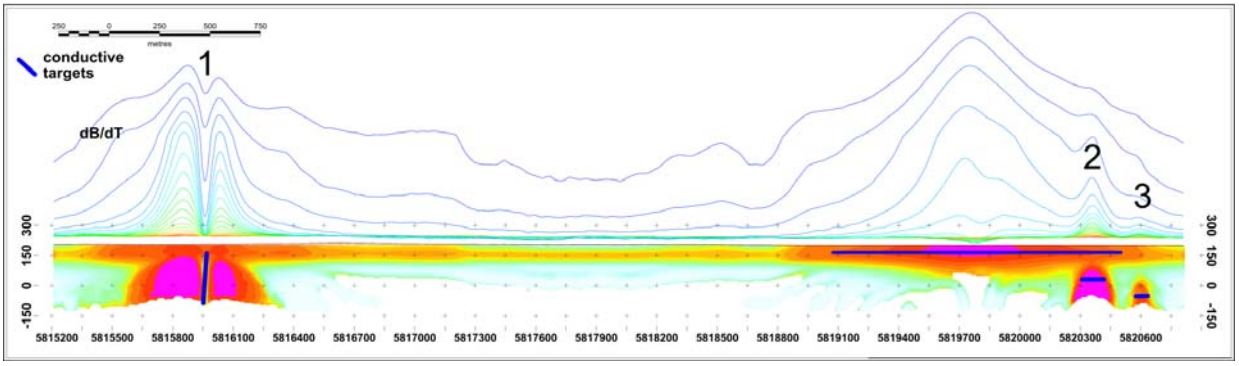

Figure E-4: dB/dt profile and RDI with different depths of targets.

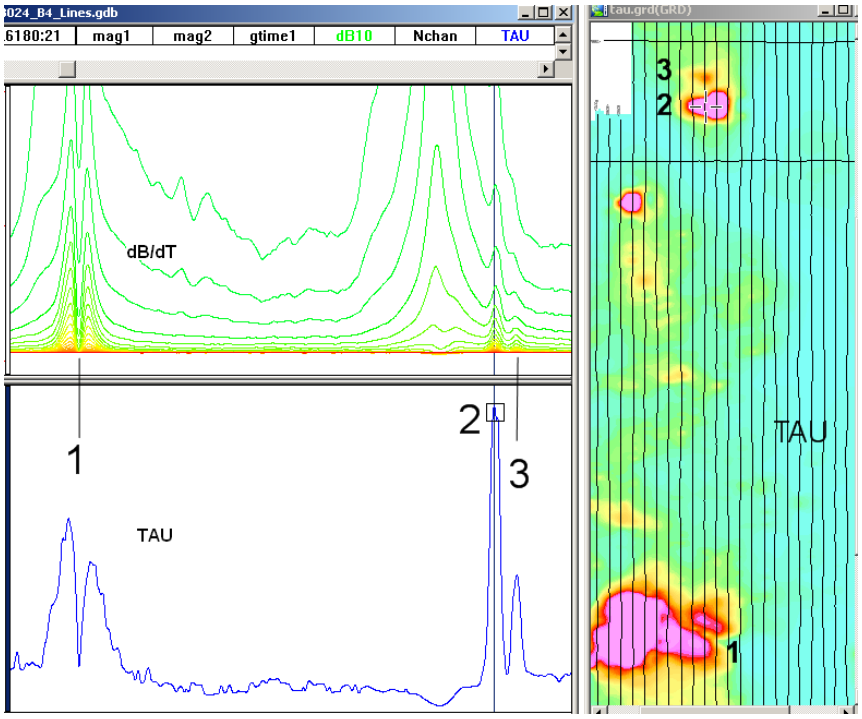

Figure E-5: Map of total TAU and dB/dt profile.

The EM Time Constants for dB/dt and B-field were calculated using the "sliding Tau" in-house program developed at Geotech2. The principle of the calculation is based on using of time window (4 time channels) which is sliding along the curve decay and looking for latest time channels which have a response above the level of noise and decay. The EM decays are obtained from all available decay channels, starting at the latest channel. Time constants are taken from a least square fit of a straight-line (log/linear space) over the last 4 gates above a pre-set signal threshold level (Figure F6). Threshold settings are pointed in the "label" property of TAU database channels. The sliding Tau method determines that, as the amplitudes increase, the time-constant is taken at progressively later times in the EM decay. Conversely, as the amplitudes decrease, Tau is taken at progressively earlier times in the decay. If the maximum signal amplitude falls below the threshold, or becomes negative for any of the 4 time gates, then Tau is not calculated and is assigned a value of "dummy" by default.

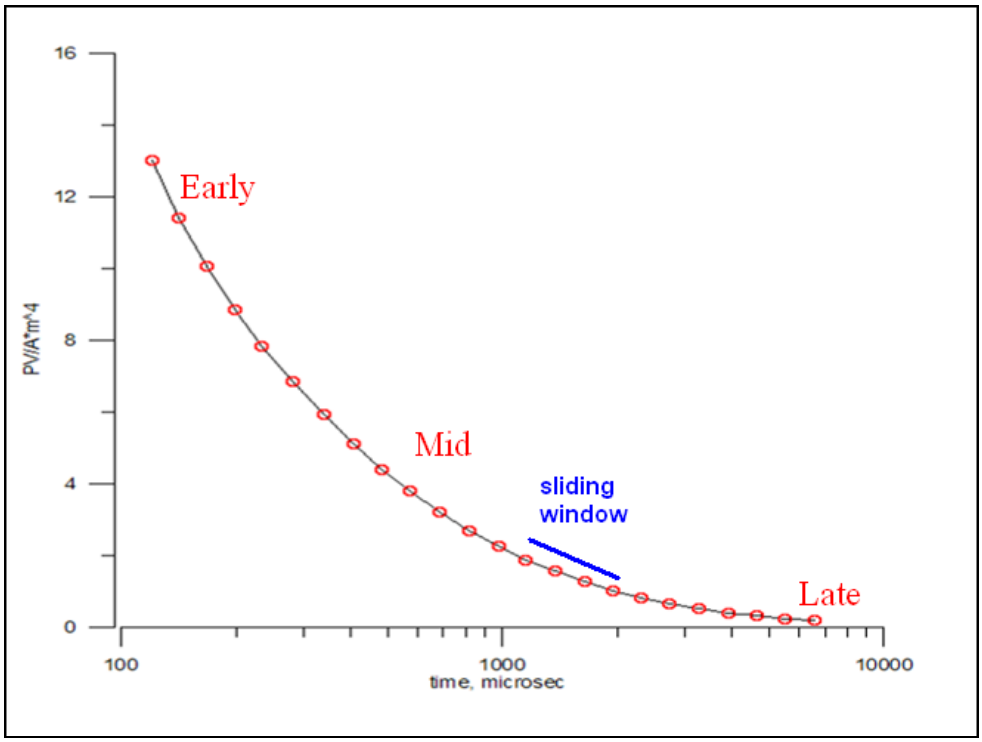

Figure E-6: Typical dB/dt decays of Vtem data

Alexander Prikhodko, PhD, P.Geo
Geotech Ltd.

September 2010

[2] by A.Prikhodko

APPENDIX F

TEM RESISTIVITY DEPTH IMAGING (RDI)

Resistivity depth imaging (RDI) is technique used to rapidly convert EM profile decay data into an equivalent resistivity versus depth cross-section, by deconvolving the measured TEM data.
The used RDI algorithm of Resistivity-Depth transformation is based on scheme of the apparent resistivity transform of Maxwell A.Meju (1998)[1] and TEM response from conductive half-space. The program is developed by Alexander Prikhodko and depth calibrated based on forward plate modeling for VTEM system configuration (Fig. 1-10).

RDIs provide reasonable indications of conductor relative depth and vertical extent, as well as accurate 1D layered-earth apparent conductivity/resistivity structure across VTEM flight lines. Approximate depth of investigation of a TEM system, image of secondary field distribution in half space, effective resistivity, initial geometry and position of conductive targets is the information obtained on base of the RDIs.

Maxwell forward modeling with RDI sections from the synthetic responses (VTEM system)

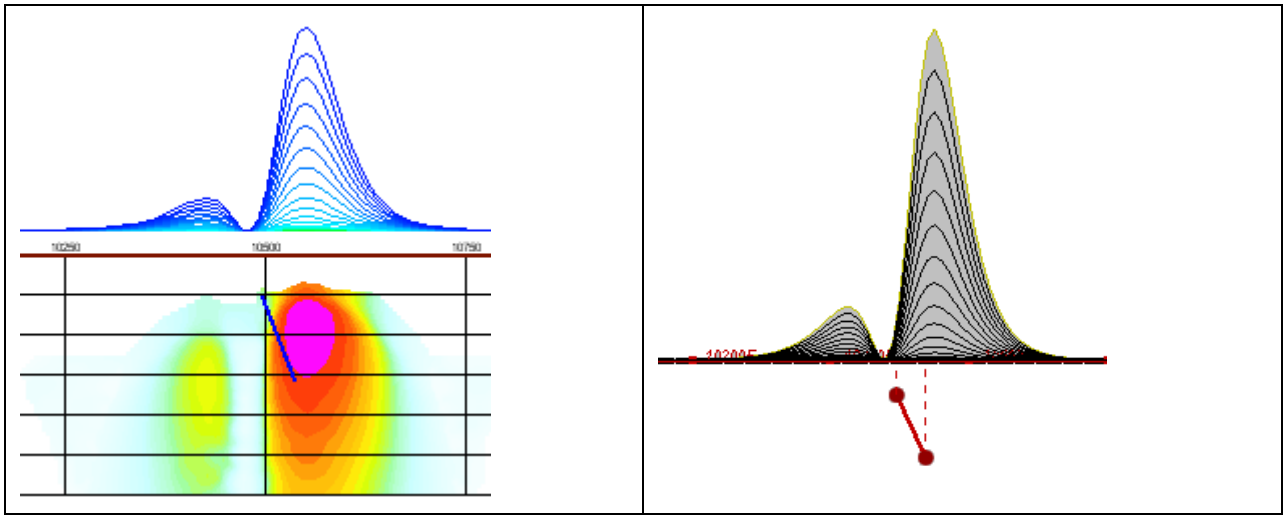

Figure F-1: Maxwell plate model and RDI from the calculated response for conductive “thin” plate (depth 50 m, dip 65 degree, depth extend 100 m).

[1] Maxwell A.Meju, 1998, Short Note: A simple method of transient electromagnetic data analysis, Geophysics, **63**, 405–410.

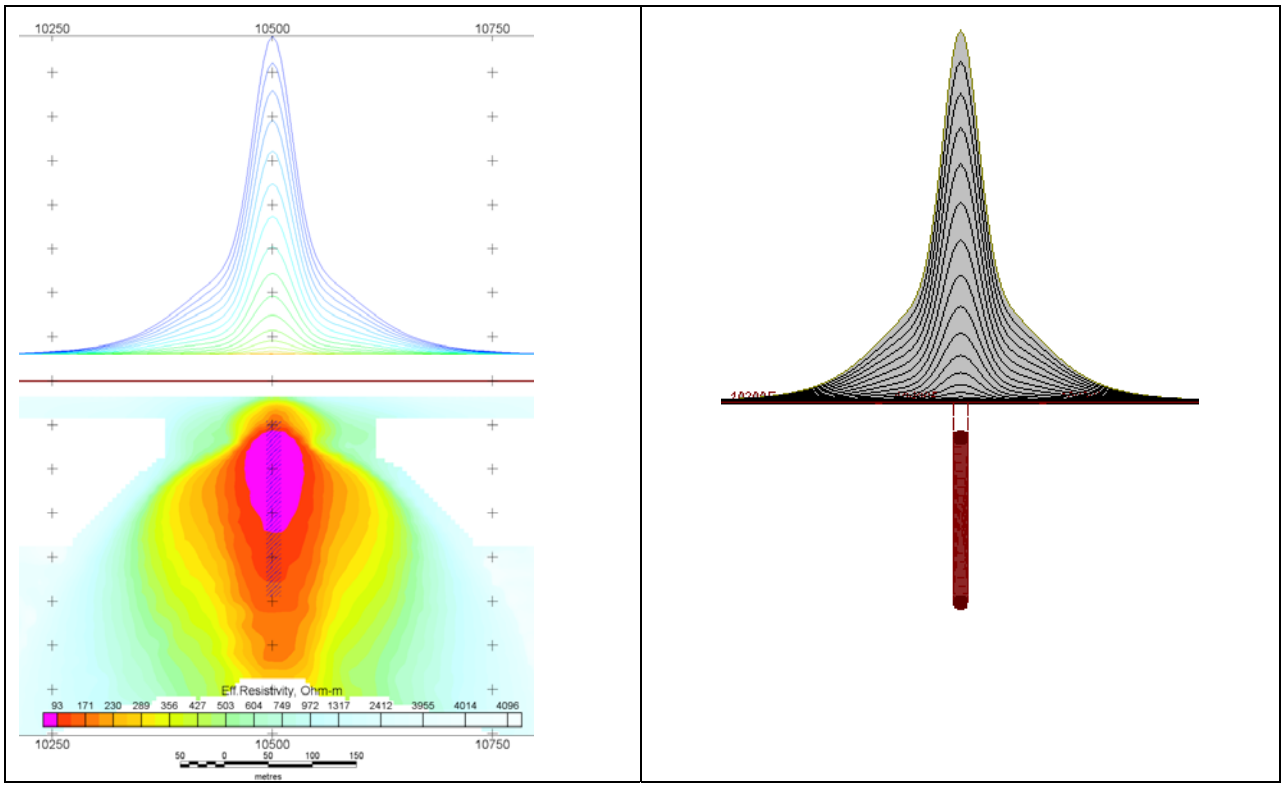

Figure F-2: Maxwell plate model and RDI from the calculated response for "thick" plate 18 m thickness, depth 50 m, depth extend 200 m).

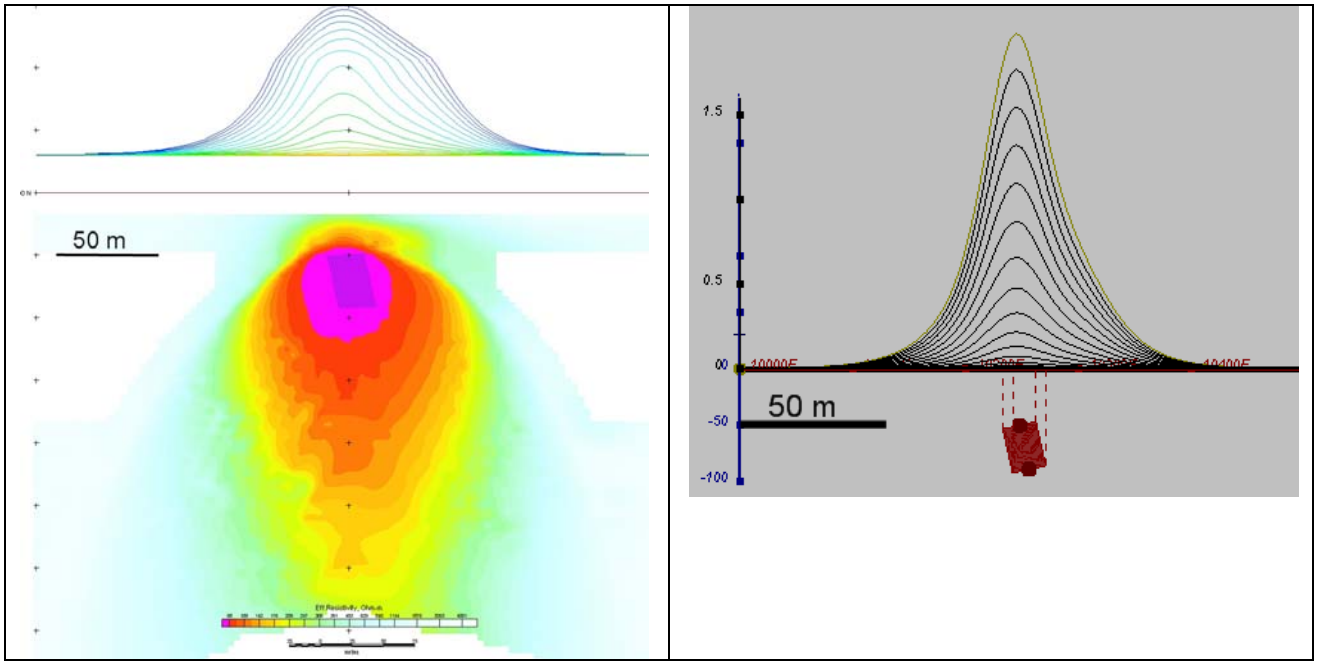

Figure F-3: Maxwell plate model and RDI from the calculated response for bulk ("thick") 100 m length, 40 m depth extend, 30 m thickness

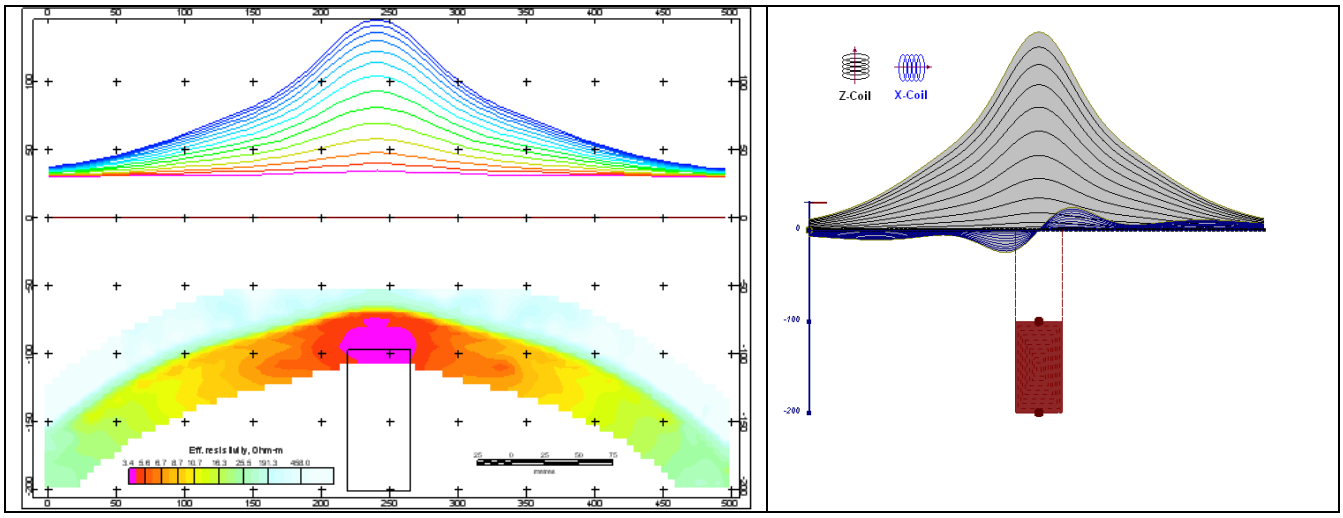

Figure F-4: Maxwell plate model and RDI from the calculated response for “thick” vertical target (depth 100 m, depth extend 100 m). 19-44 chan.

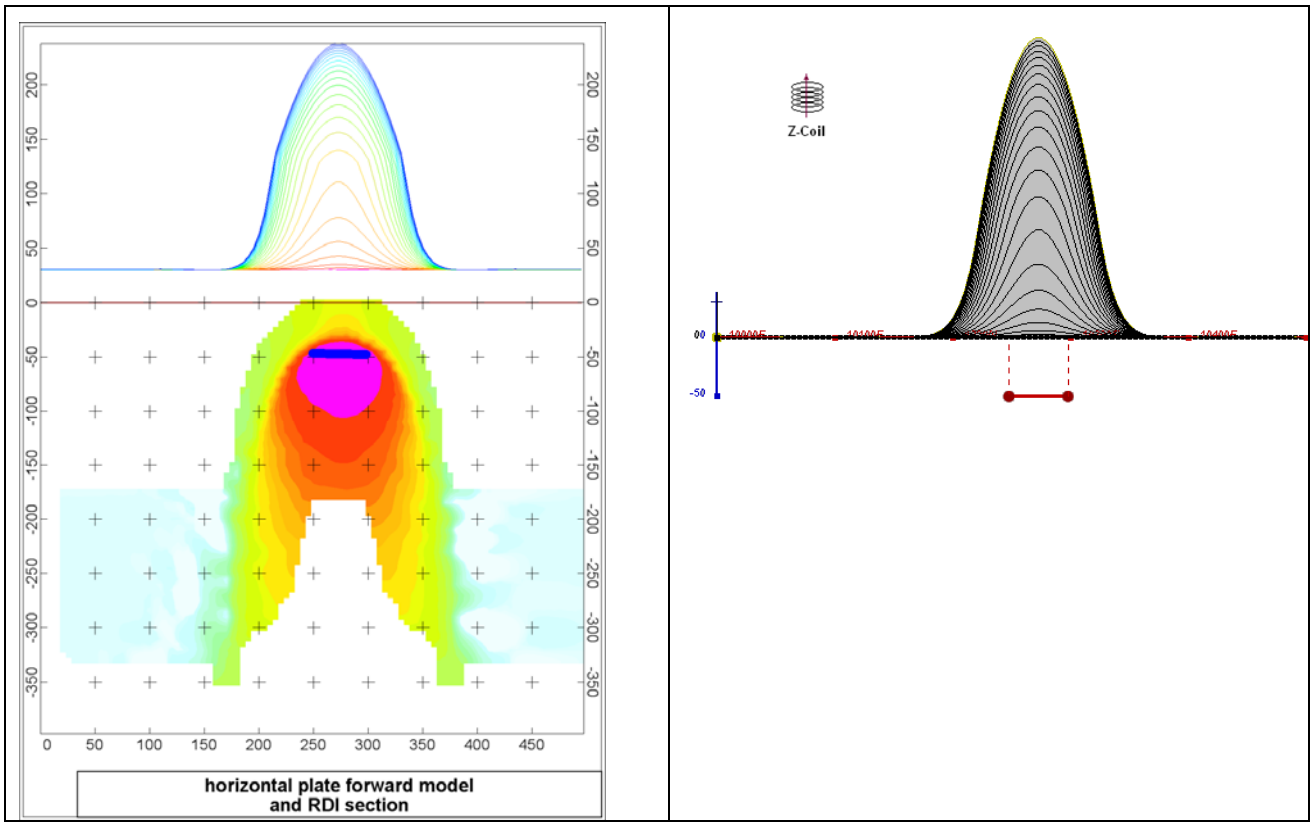

Figure F-5: Maxwell plate model and RDI from the calculated response for horizontal thin plate (depth 50 m, dim 50x100 m). 15-44 chan.

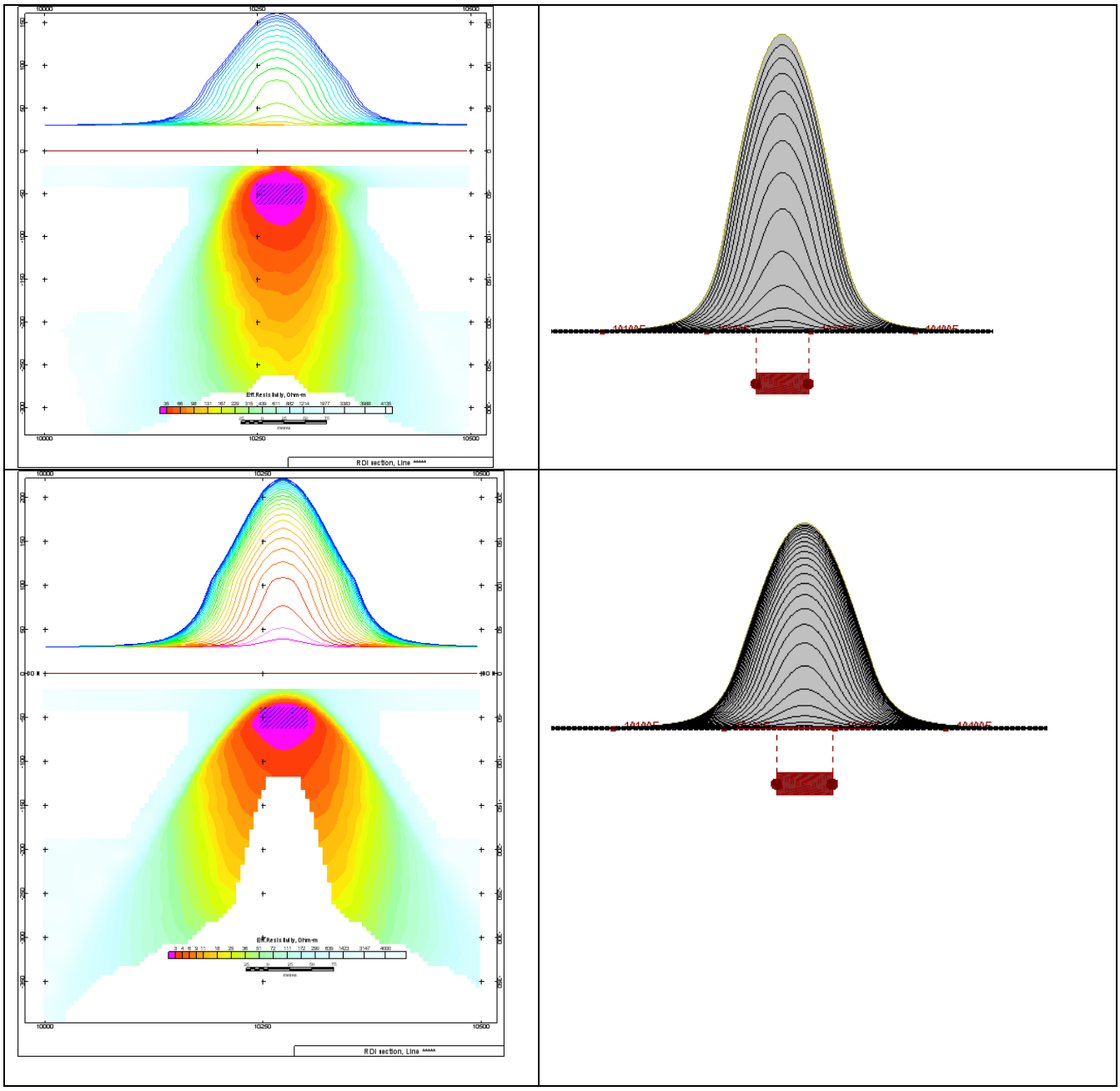

Figure F-6: Maxwell plate model and RDI from the calculated response for horizontal thick (20m) plate – less conductive (on the top), more conductive (below)

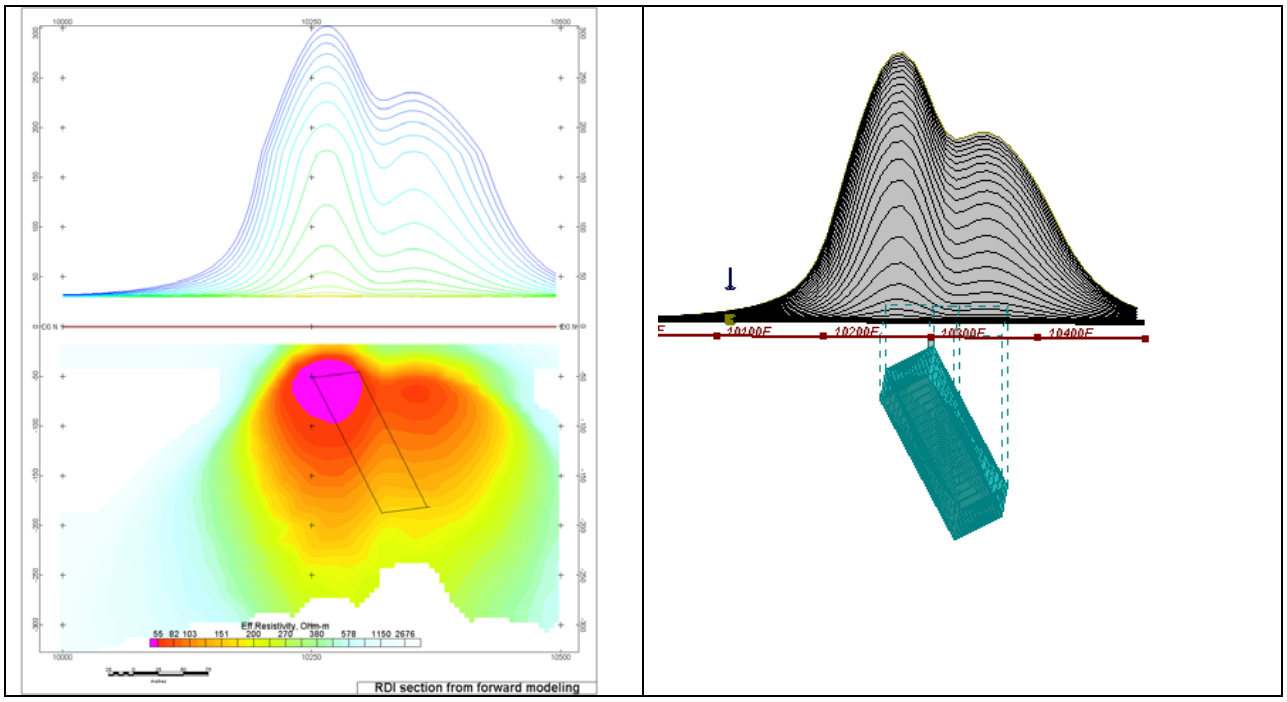

Figure F-7: Maxwell plate model and RDI from the calculated response for inclined thick (50m) plate. Depth extends 150 m, depth to the target 50 m.

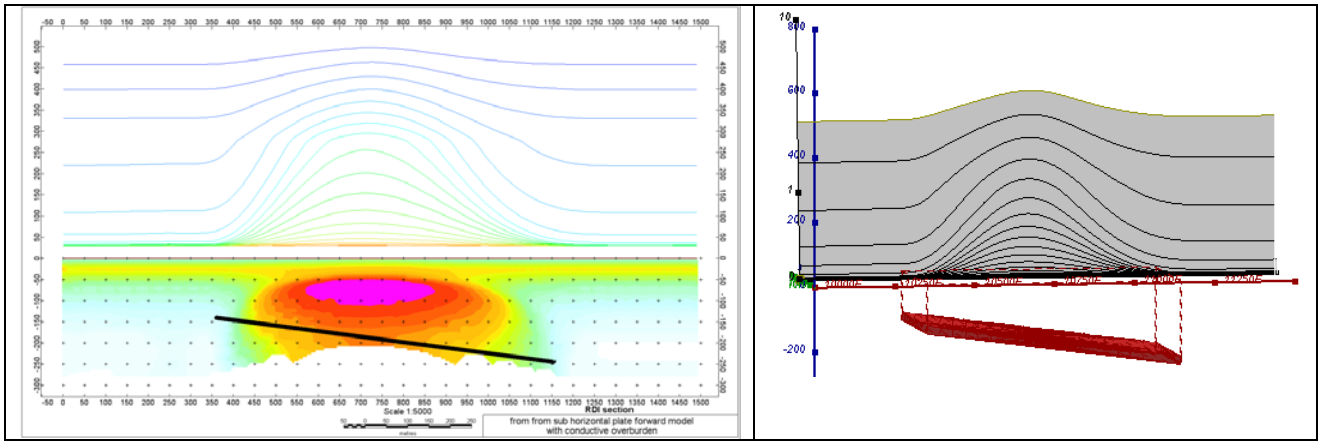

Figure F-8: Maxwell plate model and RDI from the calculated response for the long, wide and deep subhorizontal plate (depth 140 m, dim 25x500x800 m) with conductive overburden.

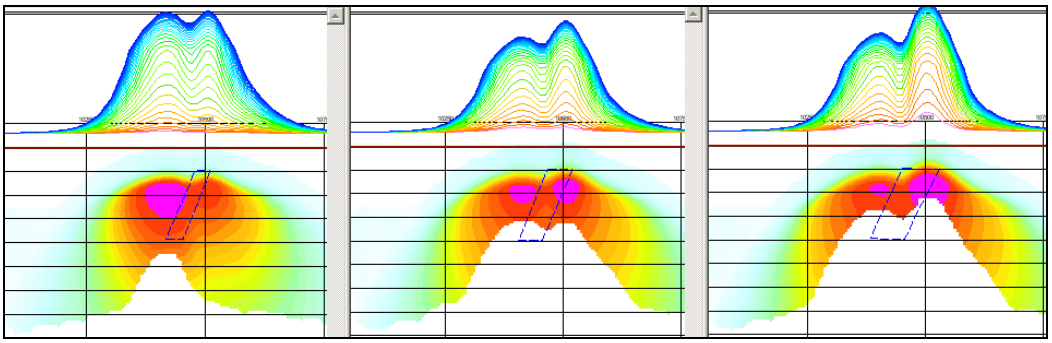

Figure F-9: Maxwell plate models and RDIs from the calculated response for "thick" dipping plates (35, 50, 75 m thickness), depth 50 m, conductivity 2.5 S/m.

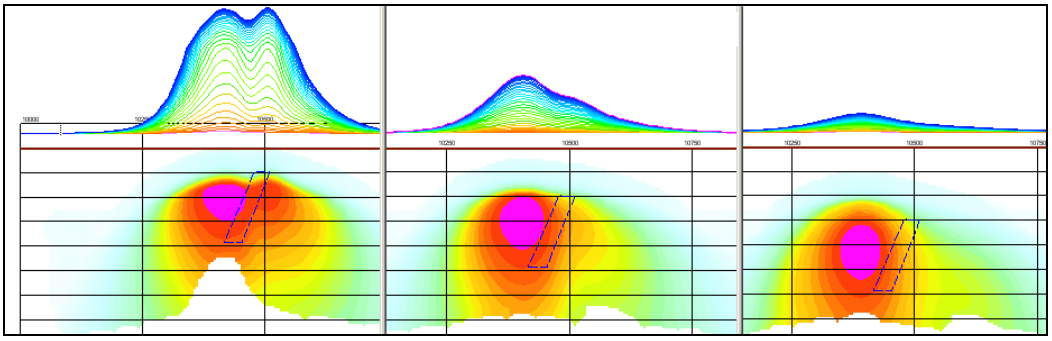

Figure F-10: Maxwell plate models and RDIs from the calculated response for "thick" (35 m thickness) dipping plate on different depth (50, 100, 150 m), conductivity 2.5 S/m.

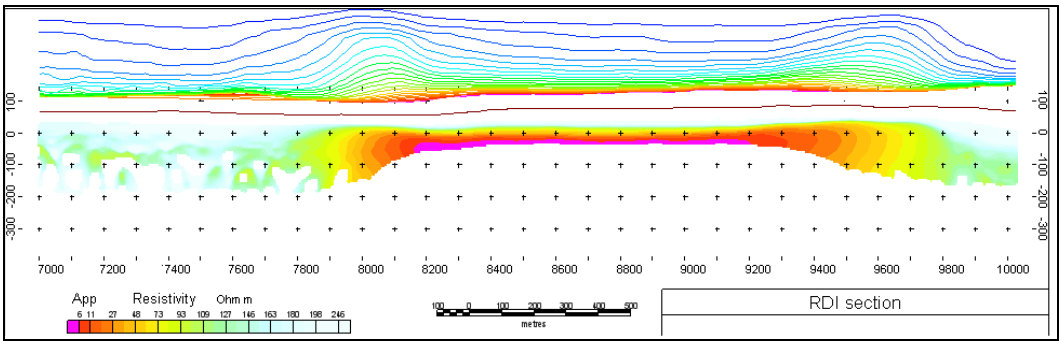

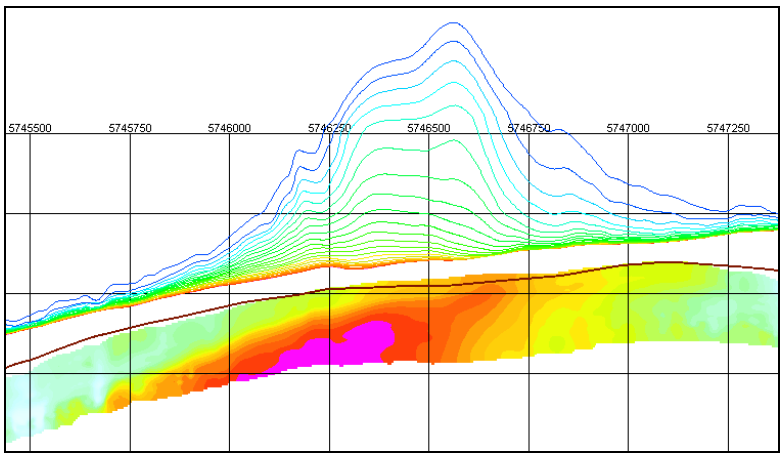

Figure F-11: RDI section for the real horizontal and slightly dipping conductive layers

FORMS OF RDI PRESENTATION

Presentation of series of lines

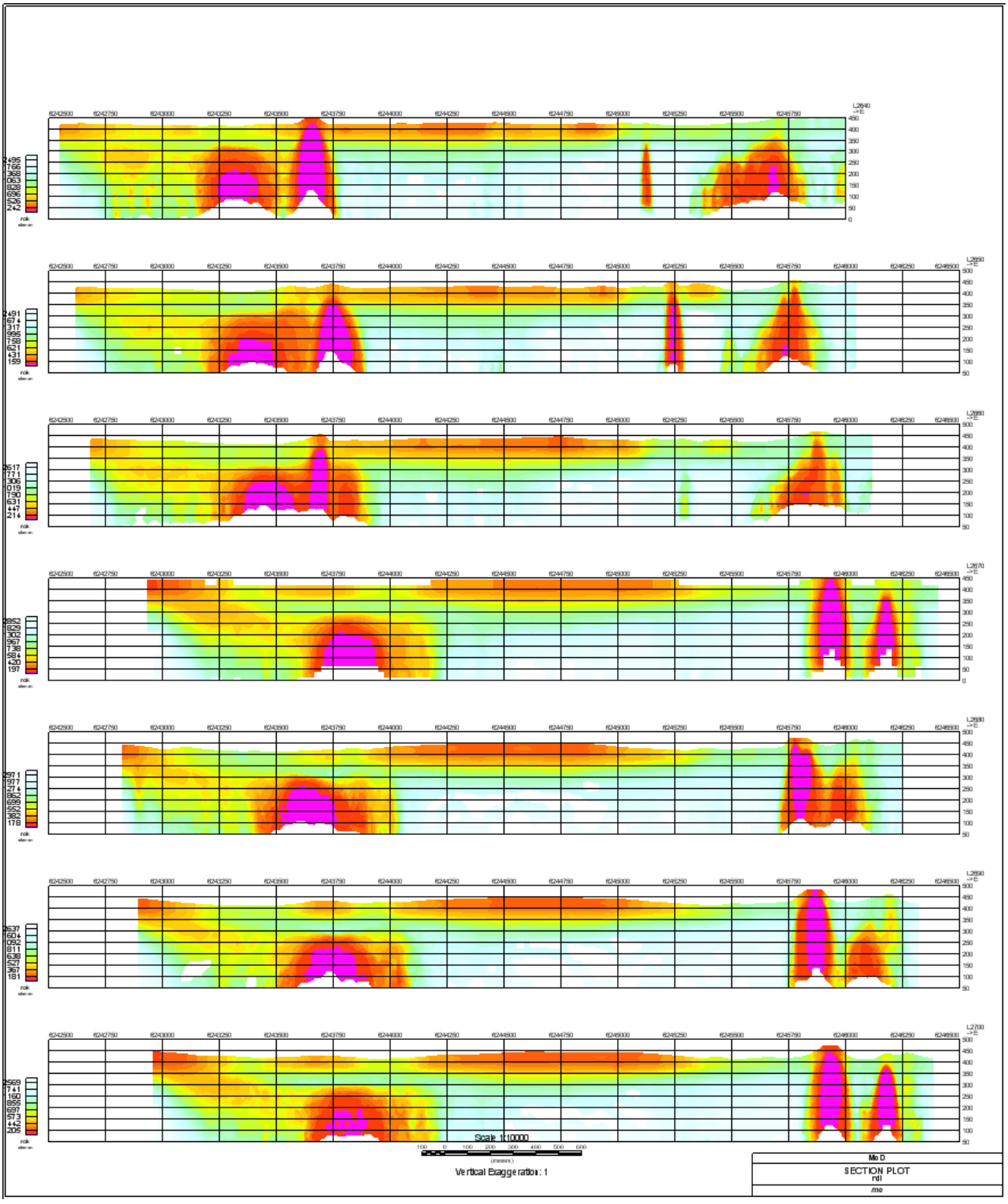

3d presentation of RDIs

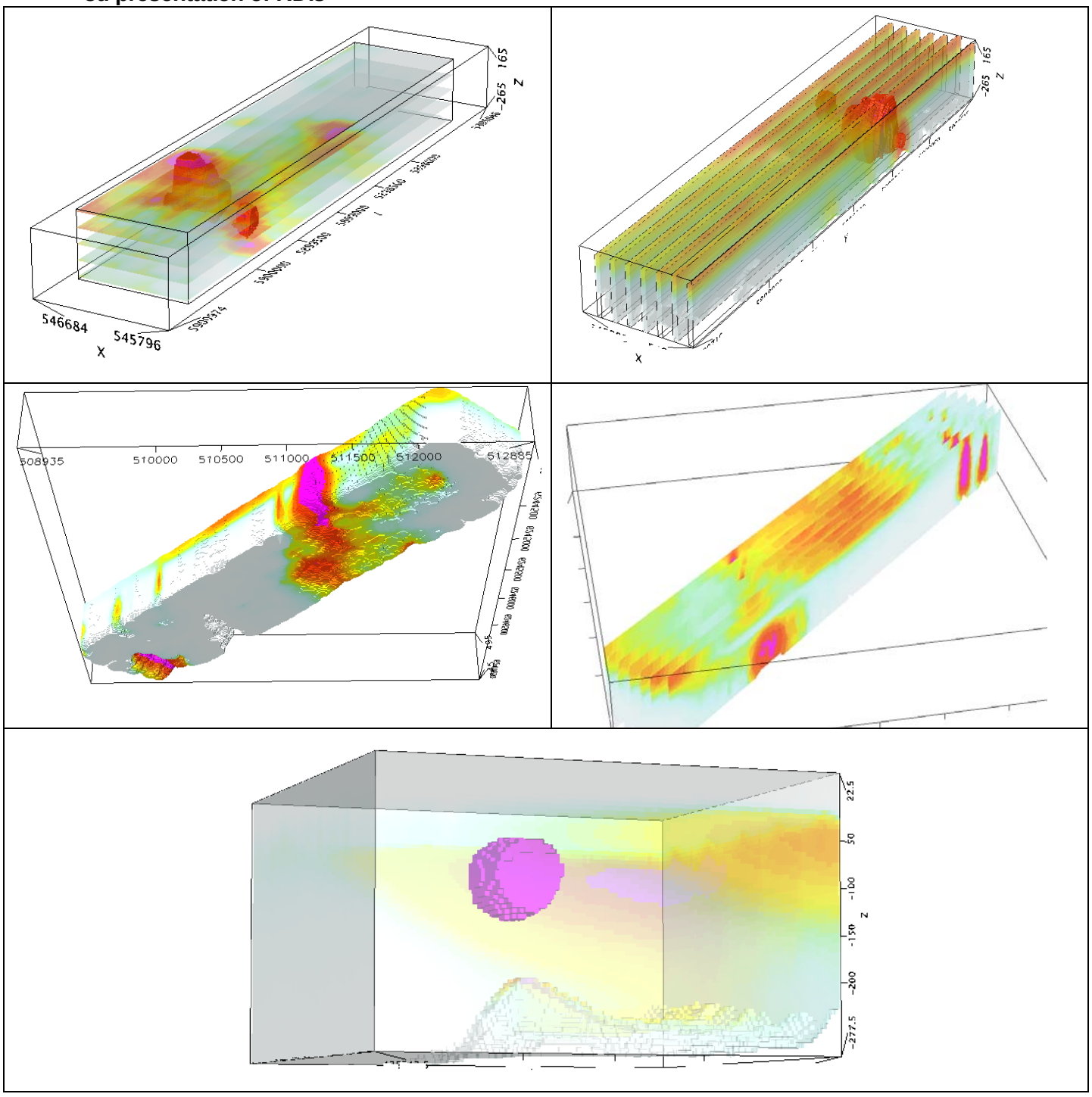

Apparent Resistivity Depth Slices plans:

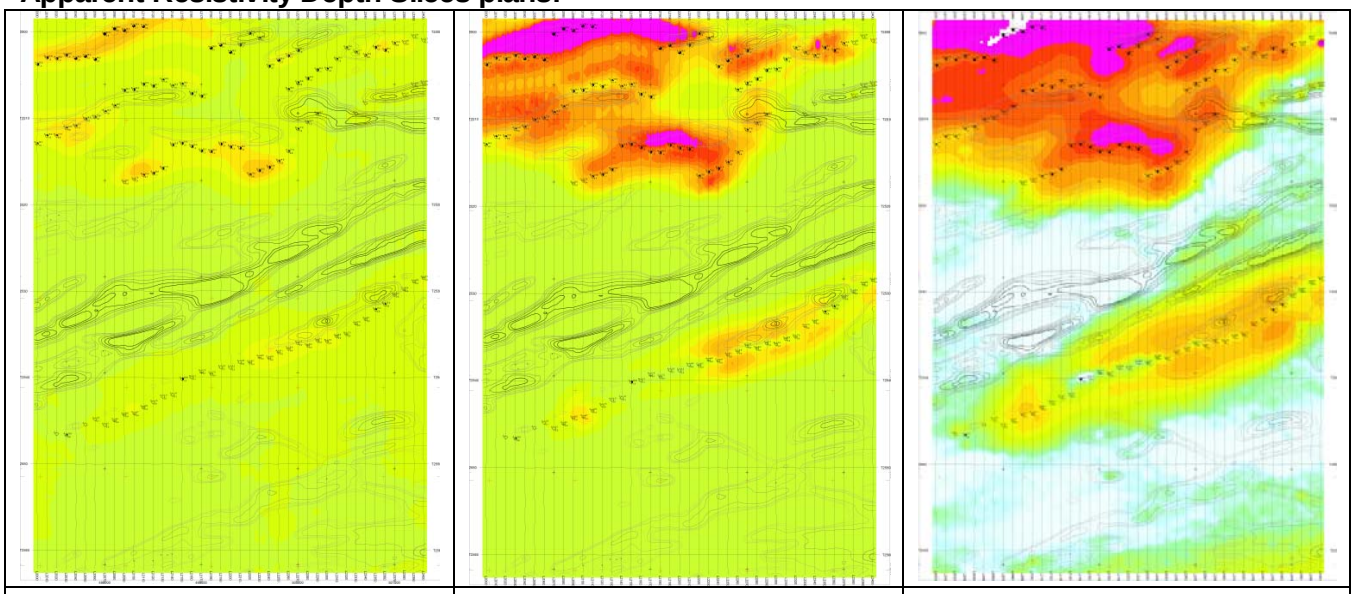

0 m (surface)	-100 m	-200 m

3d views of apparent resistivity depth slices:

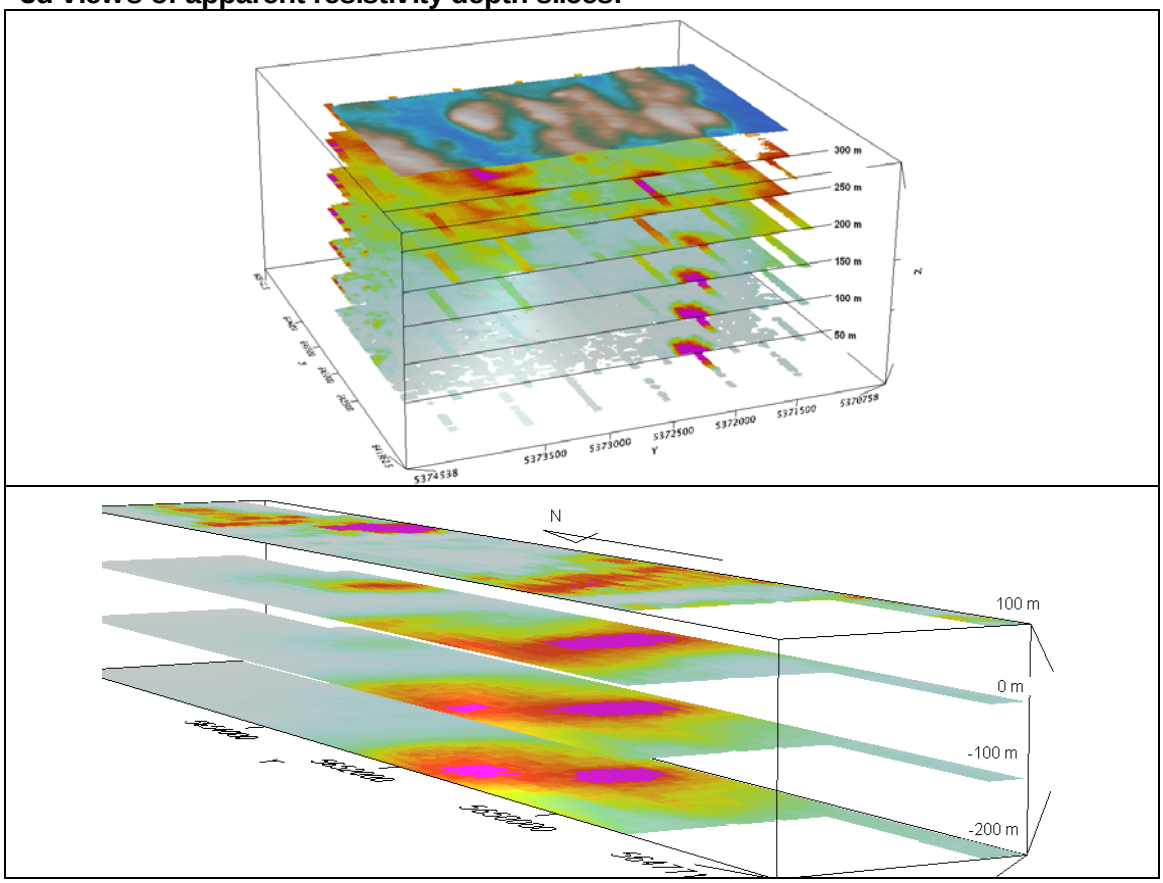

Real base metal targets in comparison with RDIs:

RDI section of the line over Caber deposit ("thin" subvertical plate target and conductive overburden.

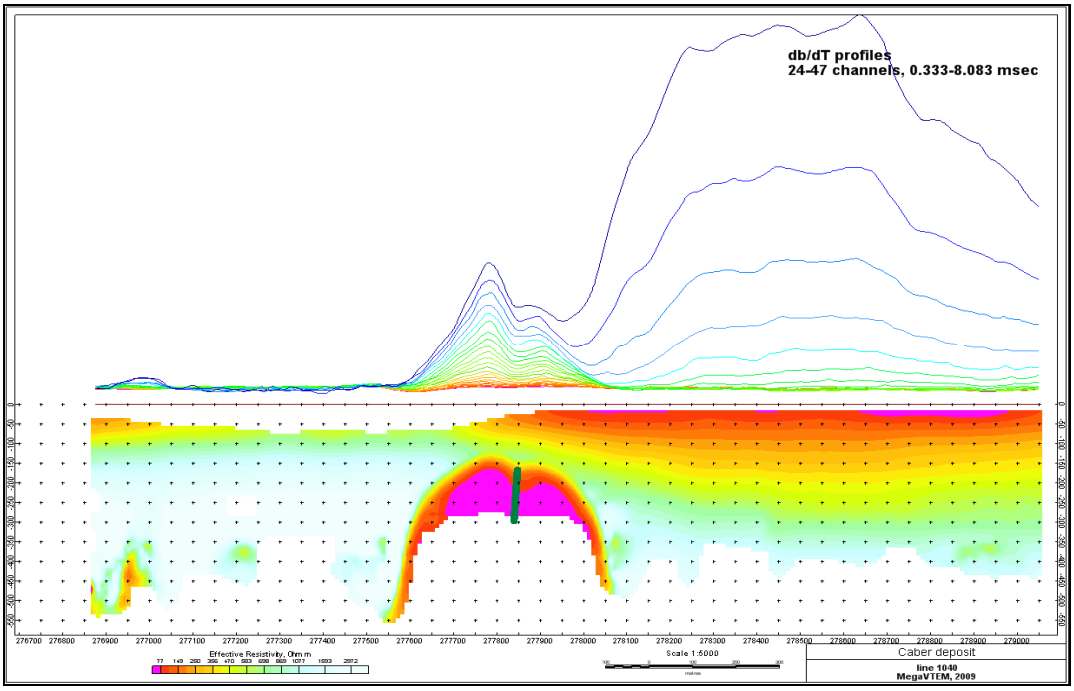

3d RDI voxels with base metals ore bodies (Middle East):

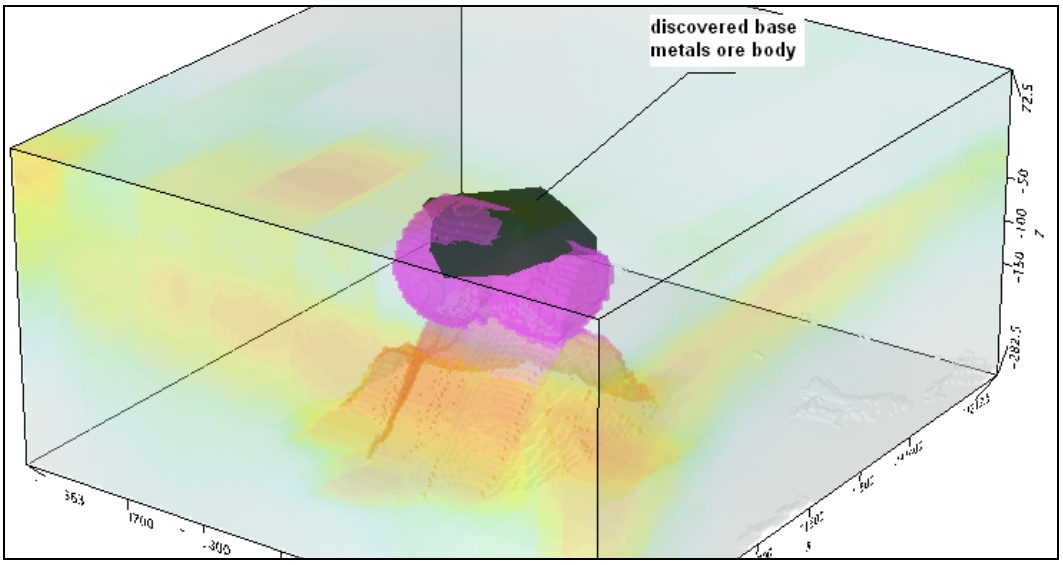

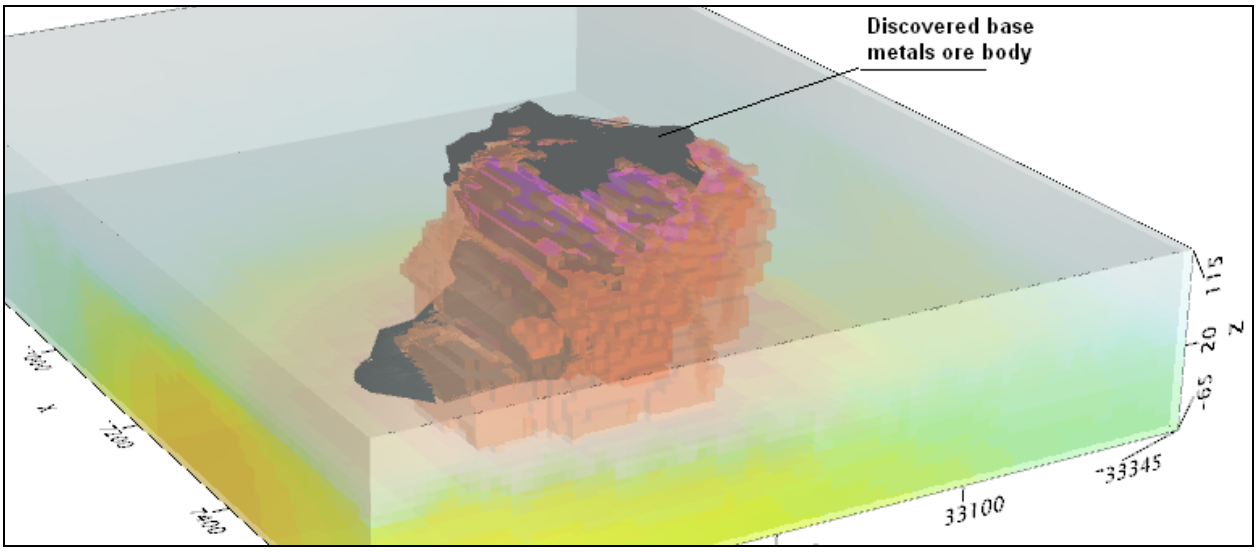

Alexander Prikhodko, PhD, P.Geo
Geotech Ltd.
April 2011